Studies of Electroweak Interactions via Vector Boson Scattering at the ATLAS Detector

Gia Khoriauli

University of Würzburg

DPG-Frühjahrstagung 2024

Karlsruhe 05.06.2024

Electroweak Multiboson Interactions

- The Standard Model (SM) of elementary particles predicts triple and quartic gauge couplings between the electroweak bosons due to the non-Abelian structure of the electroweak interaction

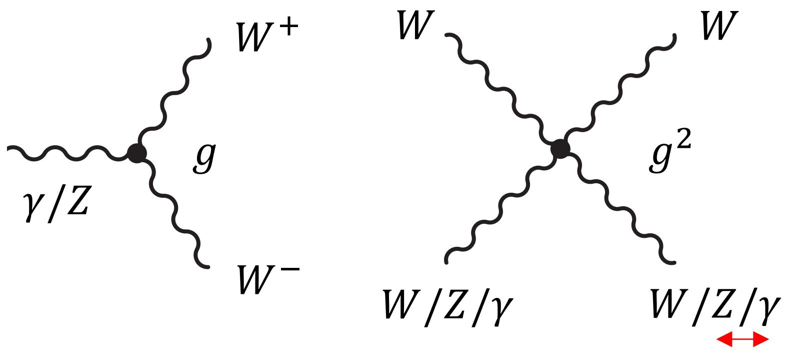

Electroweak Multiboson Interactions

- The Standard Model (SM) of elementary particles predicts triple and quartic gauge couplings between the electroweak bosons due to the non-Abelian structure of the electroweak interaction

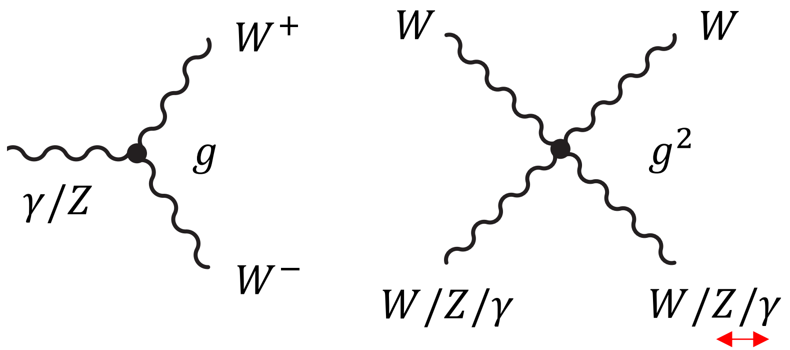

- Heavy vector bosons couple with the SM Higgs boson

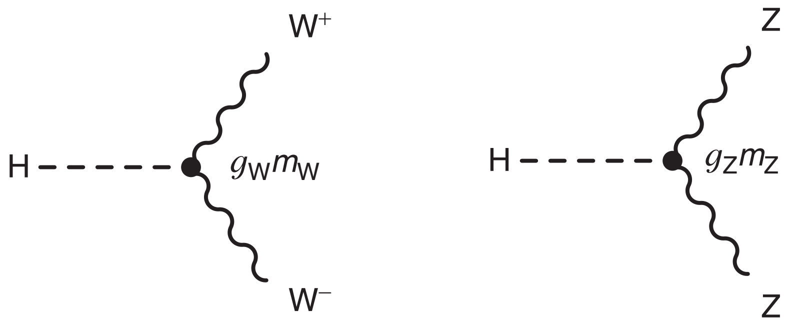

Electroweak Multiboson Interactions

- The Standard Model (SM) of elementary particles predicts triple and quartic gauge couplings between the electroweak bosons due to the non-Abelian structure of the electroweak interaction

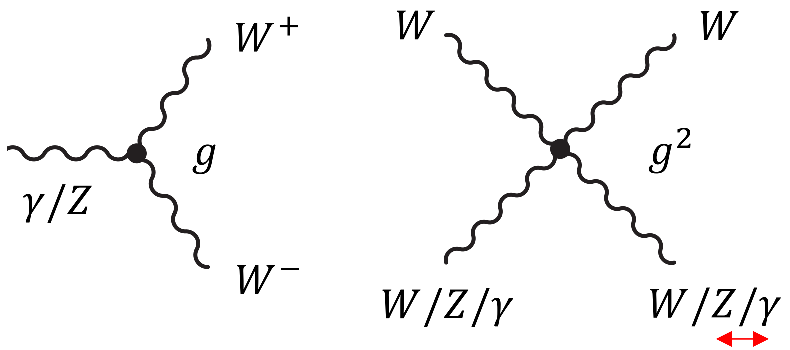

- Heavy vector bosons couple with the SM Higgs boson

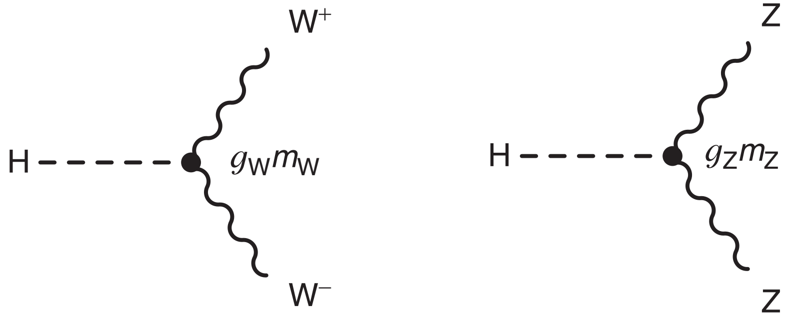

- Experimental studies of multiboson interactions are essential tests of the electroweak gauge theory and the Standard Model Higgs mechanism of the spontaneously broken electroweak symmetry
  - Fiducial and differential cross sections, effective field theory interpretations, etc.

Electroweak Vector Boson Scattering

- Electroweak VBS processes $\boldsymbol{V_1 V_2 \rightarrow V_3 V_4}$ have not been studied experimentally before the LHC experiments
  - Initial state electroweak bosons radiated from colliding quarks in pp-collisions
  - Low production cross sections (~ fb) even at the LHC energies
    - → sensitive to possible new physics effects leading to anomalous quartic gauge couplings

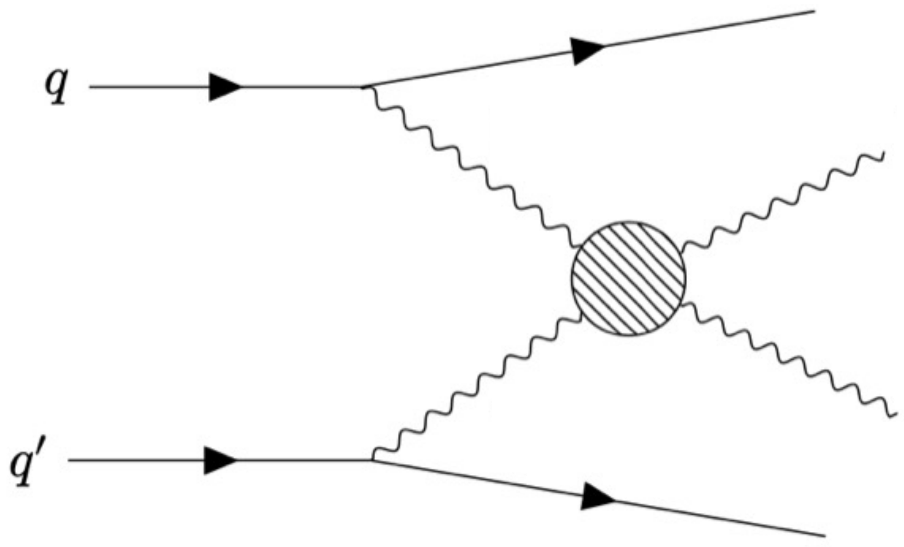

Electroweak Vector Boson Scattering

- Electroweak VBS processes $\boldsymbol{V_1\,V_2 \rightarrow V_3\,V_4}$ have not been studied experimentally before the LHC experiments
  - Initial state electroweak bosons radiated from colliding quarks in pp-collisions
  - Low production cross sections (~ fb) even at the LHC energies
    - → sensitive to possible new physics effects leading to anomalous quartic gauge couplings

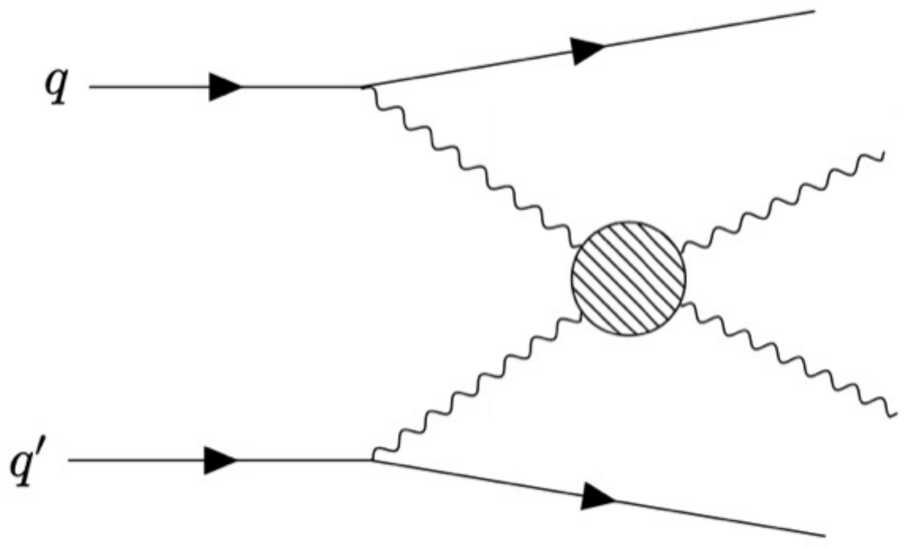

- Depending on the vector boson actors, V_1, V_2, V_3 and V_4 of the scattering process, it can involve all or some of the leading order diagrams presented below

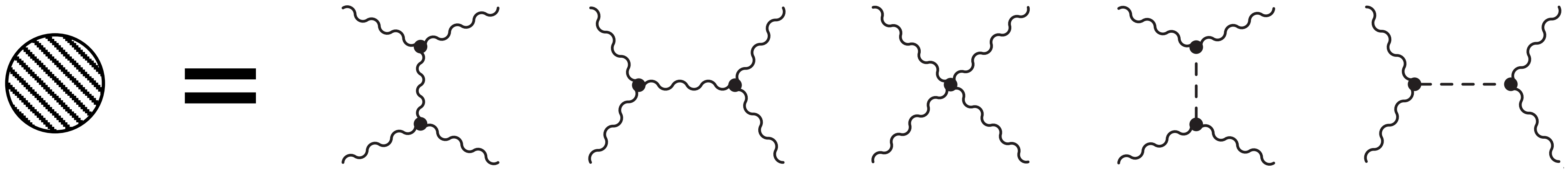

$VVjj$ Production with $V = W, Z, \gamma$ at Leading Order

- Pure EW & s-/t-channel production with the Higgs boson propagator

VBS

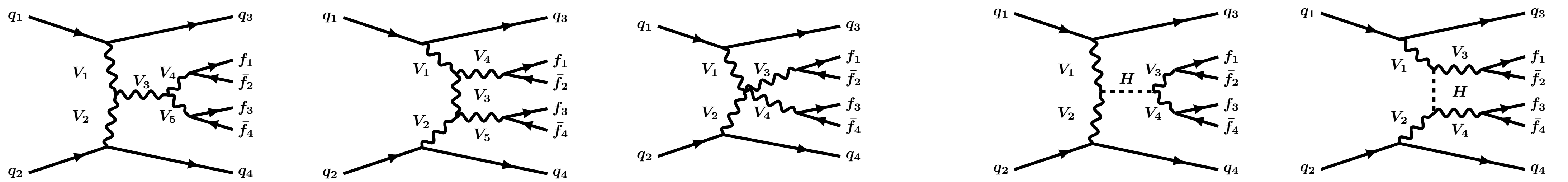

$VVjj$ Production with $V = W, Z, \gamma$ at Leading Order

- ❑ Pure EW & s-/t-channel production with the Higgs boson propagator

VBS

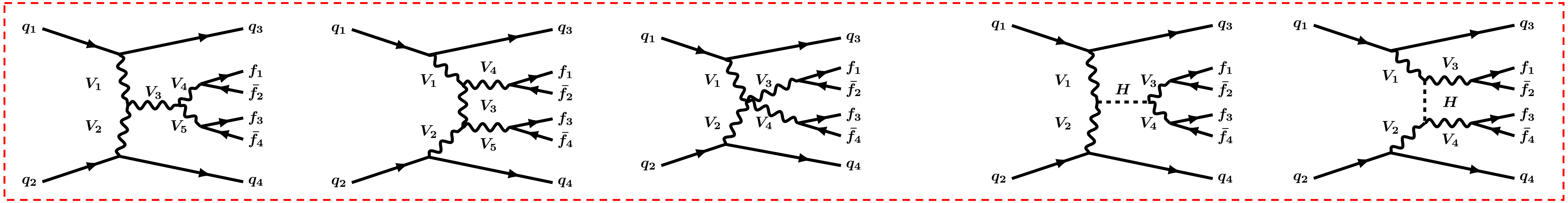

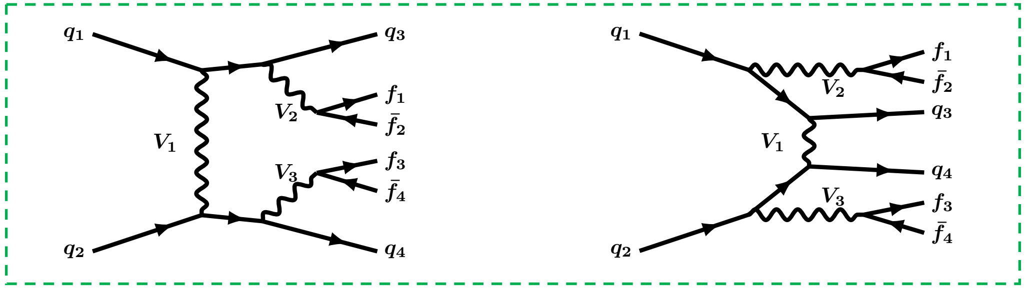

Radiative

$VVjj$ Production with $V = W, Z, \gamma$ at Leading Order

- Pure EW & s-/t-channel production with the Higgs boson propagator

VBS

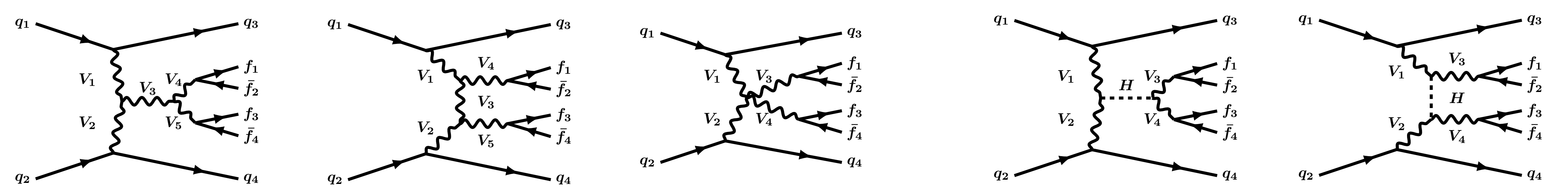

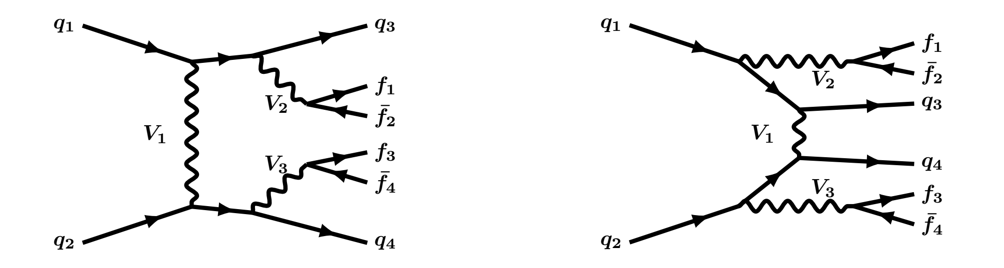

Radiative

- QCD induced production (α_S^2 - enhanced production cross sections)

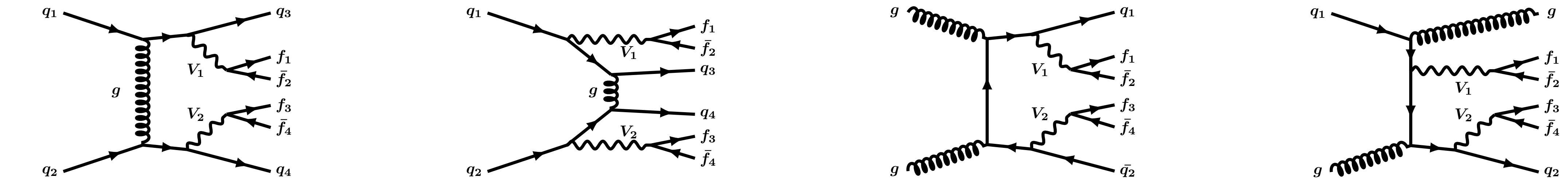

VBS and Electroweak Symmetry Breaking Mechanism

- The SM massive electroweak bosons obtain their masses and longitudinal polarisations via the Higgs mechanism of the spontaneously broken electroweak symmetry
  - Measurements of polarisation observables in the multiboson interactions are the direct probes of this mechanism

VBS and Electroweak Symmetry Breaking Mechanism

- The SM massive electroweak bosons obtain their masses and longitudinal polarisations via the Higgs mechanism of the spontaneously broken electroweak symmetry
  - Measurements of polarisation observables in the multiboson interactions are the direct probes of this mechanism
- Diagrams with Higgs boson are crucial to avoid the unitarity violation due to the rising scattering cross section of longitudinally polarized W bosons: $\boldsymbol{W_L W_L \rightarrow W_L W_L}$

A. Denner & T. Hahn, Nucl.Phys.B525:27–50,1998

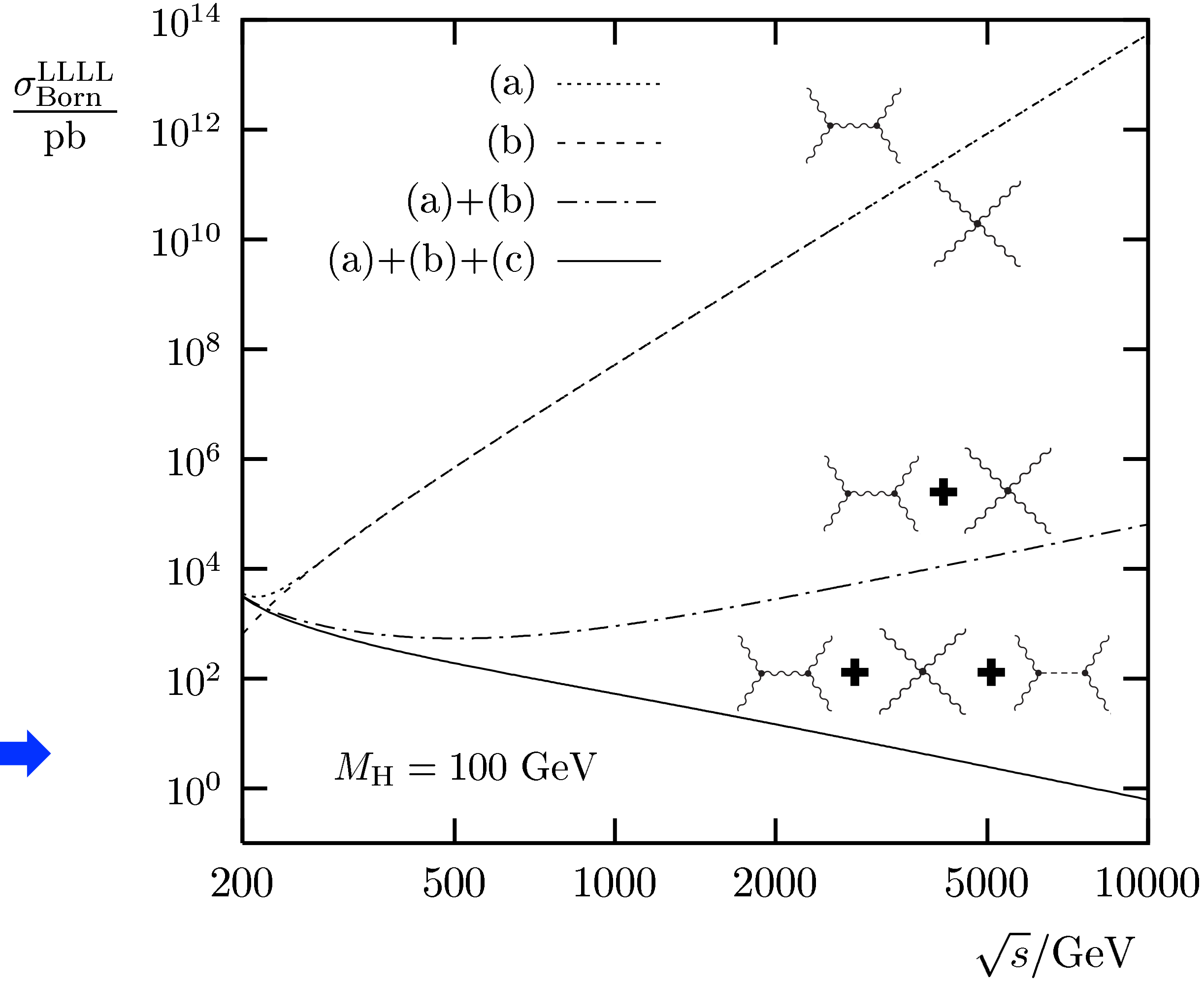

Searches for New Physics Effects

- No non-SM particles & resonances are discovered at the LHC so far

- If there are any, their masses are likely beyond the reach of the LHC energy

- They can still cause measurable effects on some physics observables as virtual particles

Searches for New Physics Effects

- ❑ No non-SM particles & resonances are discovered at the LHC so far

- ❑ If there are any, their masses are likely beyond the reach of the LHC energy

- ❑ They can still cause measurable effects on some physics observables as virtual particles

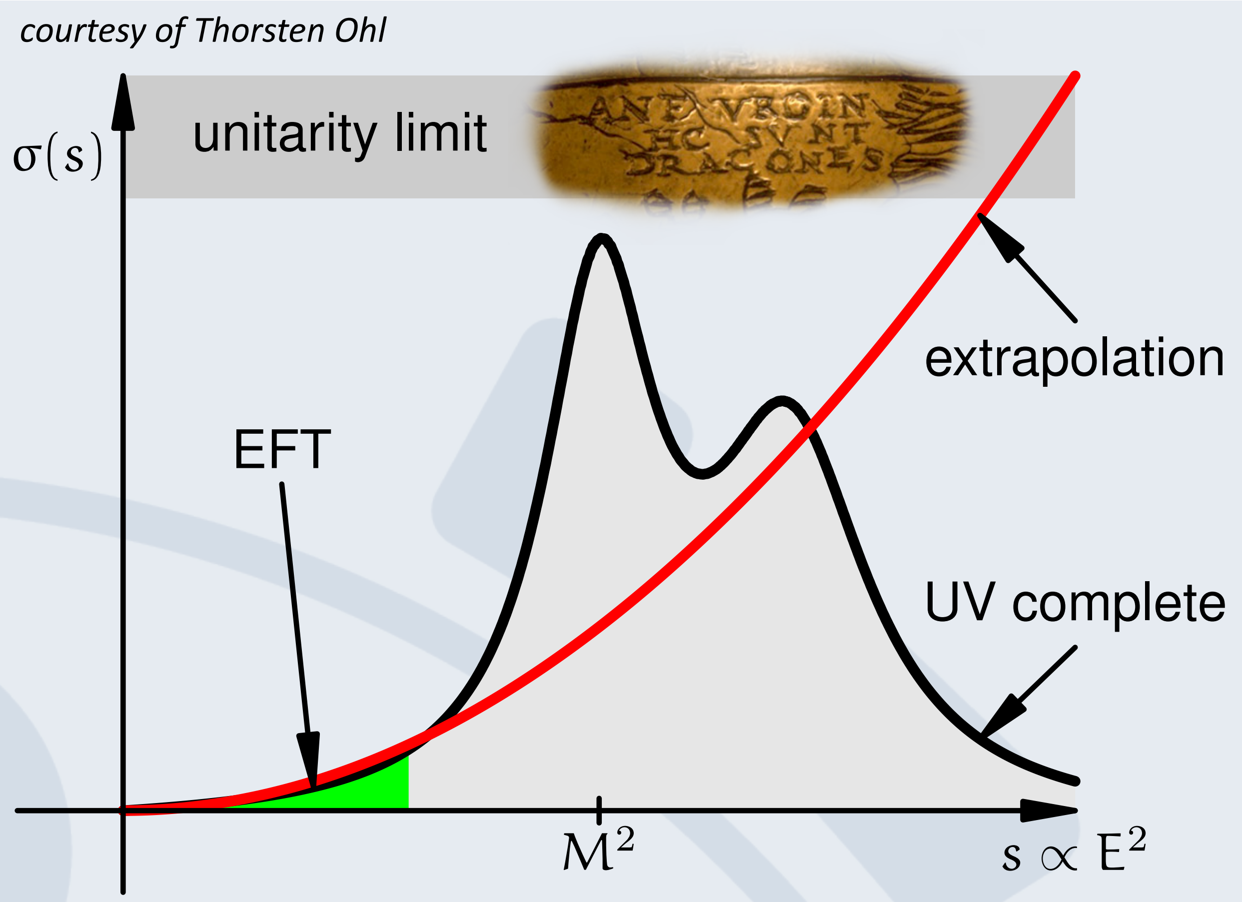

- ❑ Searches for those effects are normally performed in model-independent ways using effective field theory (EFT) frameworks

Searches for New Physics Effects with EFT Parameterisation

- ❑ Low energy effective field theory to parameterize new physics effects with the help of high dimension (n>4) operators $\mathcal{O}_i^{(n)}$
  - ❖ Linear realization of the SM $SU(2)_L \otimes U(1)_Y$ gauge symmetry

$$\mathcal{L}_{\text{eff}} = \mathcal{L}_{\text{SM}} + \sum_{n=5}^{\infty} \sum_i \frac{f_i^{(n)}}{\Lambda^{n-4}} \mathcal{O}_i^{(n)}$$

Eboli et al., 2020

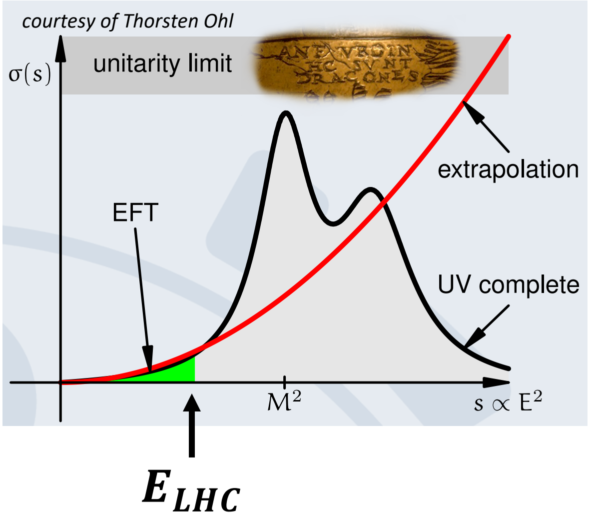

Searches for New Physics Effects with EFT Parameterisation

- Low energy effective field theory to parameterize new physics effects with the help of high dimension (n>4) operators $\mathcal{O}_i^{(n)}$
  - Linear realization of the SM $SU(2)_L \otimes U(1)_Y$ gauge symmetry

$$\mathcal{L}_{\text{eff}} = \mathcal{L}_{\text{SM}} + \sum_{n=5}^{\infty} \sum_{i} \frac{f_i^{(n)}}{\Lambda^{n-4}} \mathcal{O}_i^{(n)}$$

Eboli et al., 2020

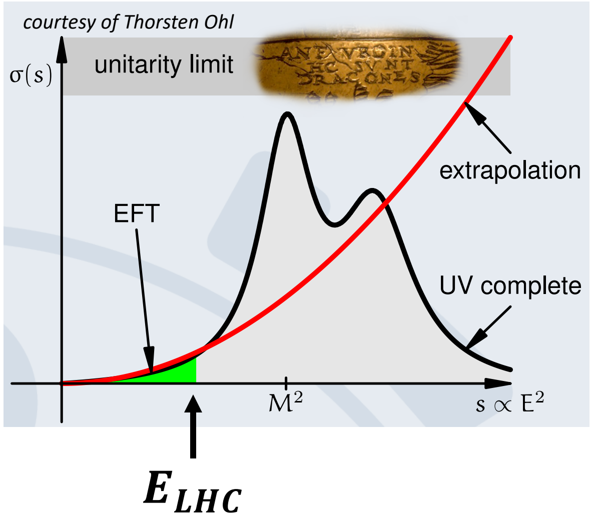

- Some dimension-6 and 8 operators are interesting in multiboson measurements as they generate anomalous triple and quartic gauge couplings, aTGC and aQGC

$$\mathcal{L}_{\text{eff}} = \mathcal{L}_{\text{SM}} + \sum_i \frac{f_i^{(6)}}{\Lambda^2} O_i + \sum_j \frac{f_j^{(8)}}{\Lambda^4} O_j + \ldots$$

Searches for New Physics Effects with EFT Parameterisation

- ❑ Low energy effective field theory to parameterize new physics effects with the help of high dimension (n>4) operators $\mathcal{O}_i^{(n)}$
  - ❖ Linear realization of the SM $SU(2)_L \otimes U(1)_Y$ gauge symmetry

$$\mathcal{L}_{\text{eff}} = \mathcal{L}_{\text{SM}} + \sum_{n=5}^{\infty} \sum_i \frac{f_i^{(n)}}{\Lambda^{n-4}} \mathcal{O}_i^{(n)}$$

Eboli et al., 2020

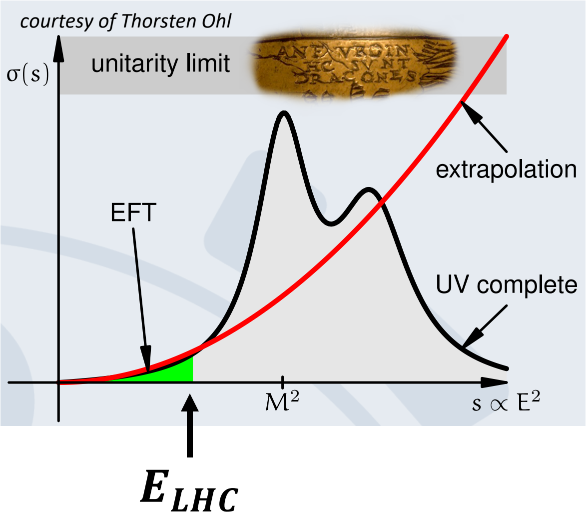

- ❑ Some dimension-6 and 8 operators are interesting in multiboson measurements as they generate anomalous triple and quartic gauge couplings, aTGC and aQGC

$$\mathcal{L}_{\text{eff}} = \mathcal{L}_{\text{SM}} + \sum_i \frac{f_i^{(6)}}{\Lambda^2} O_i + \sum_j \frac{f_j^{(8)}}{\Lambda^4} O_j + \dots$$

- ❑ Lowest order operators that generate aQGC but not aTGC are dimension-8 operators

Degrande et al., 2013

	WWWW	WWZZ	ZZZZ	WWAZ	WWAA	ZZZA	ZZAA	ZAAA	AAAA
$\mathcal{O}_{S,0}$, $\mathcal{O}_{S,1}$	X	X	X						
$\mathcal{O}_{M,0}$, $\mathcal{O}_{M,1}$, $\mathcal{O}_{M,6}$, $\mathcal{O}_{M,7}$	X	X	X	X	X	X	X		
$\mathcal{O}_{M,2}$, $\mathcal{O}_{M,3}$, $\mathcal{O}_{M,4}$, $\mathcal{O}_{M,5}$		X	X	X	X	X	X		
$\mathcal{O}_{T,0}$, $\mathcal{O}_{T,1}$, $\mathcal{O}_{T,2}$	X	X	X	X	X	X	X	X	X
$\mathcal{O}_{T,5}$, $\mathcal{O}_{T,6}$, $\mathcal{O}_{T,7}$		X	X	X	X	X	X	X	X
$\mathcal{O}_{T,8}$, $\mathcal{O}_{T,9}$			X			X	X	X	X

TABLE II: Quartic vertices modified by each dimension-8 operator are marked with X.

Production of EFT Samples for VBS Measurements

- ❑ EFT "model" for new physics: only dimension-8 operators have non-zero coefficients
  - ✦ (for some reason) the new physics has an effect only on the quartic gauge couplings

$$\mathcal{L}_{\mathrm{eff}} = \mathcal{L}_{\mathrm{SM}} + \sum_i \frac{\cancelto{0}{f_i^{(6)}}}{\Lambda^2} O_i + \sum_j \frac{f_j^{(8)}}{\Lambda^4} O_j + \ldots$$

- ❑ Amplitude of a VBS final state with EFT contributions: $|A_{\mathrm{SM}} + \sum_i c_i A_i|$, where $c_i = \frac{f_i^{(8)}}{\Lambda^4}$

Production of EFT Samples for VBS Measurements

- EFT "model" for new physics: only dimension-8 operators have non-zero coefficients
  - ✦ (for some reason) the new physics has an effect only on the quartic gauge couplings

$$\mathcal{L}_{\text{eff}} = \mathcal{L}_{\text{SM}} + \sum_i \underbrace{\frac{f_i^{(6)}}{\Lambda^2}}_{\to 0} O_i + \sum_j \frac{f_j^{(8)}}{\Lambda^4} O_j + \ldots$$

- Amplitude of a VBS final state with EFT contributions: $|A_{\text{SM}} + \sum_i c_i A_i|$, where $c_i = \frac{f_i^{(8)}}{\Lambda^4}$

- Standard Model, interference, quadratic and cross terms of the total squared amplitude

$$|A_{\text{SM}} + \sum_i c_i A_i|^2 = |A_{\text{SM}}|^2 + \sum_i c_i 2Re(A_{\text{SM}}^* A_i) + \sum_i {c_i}^2 |A_i|^2 + \sum_{ij, i \neq j} c_i c_j 2Re(A_i A_j^*)$$

Production of EFT Samples for VBS Measurements

- EFT "model" for new physics: only dimension-8 operators have non-zero coefficients
  - (for some reason) the new physics has an effect only on the quartic gauge couplings

$$\mathcal{L}_{\text{eff}} = \mathcal{L}_{\text{SM}} + \sum_i \cancel{\frac{f_i^{(6)}}{\Lambda^2}}^{\,0} O_i + \sum_j \frac{f_j^{(8)}}{\Lambda^4} O_j + \ldots$$

- Amplitude of a VBS final state with EFT contributions: $|A_{\text{SM}} + \sum_i c_i A_i|$, where $c_i = \frac{f_i^{(8)}}{\Lambda^4}$

- Standard Model, interference, quadratic and cross terms of the total squared amplitude

$$|A_{\text{SM}} + \sum_i c_i A_i|^2 = |A_{\text{SM}}|^2 + \sum_i c_i 2Re(A_{\text{SM}}^* A_i) + \sum_i c_i{}^2 |A_i|^2 + \sum_{ij, i \neq j} c_i c_j 2Re(A_i A_j^*)$$

- Monte-Carlo samples are generated using only individual terms at a time

- Only one c_i or one pair of c_i and c_j (for generation of cross term samples) are set to nonzero values at a time
  - Respective sample can be scaled by appropriate c_i, c_i^2, or $c_i c_j$

The ATLAS Detector

- *pp*-collision data-taking
  - **2015-2018: $\sqrt{s} = 13$ TeV**
    - $L \geq L_0,\ L_{max} = 2.1L_0$
  - 2022-2025: $\sqrt{s} = 13.6$ TeV,
    - $L = 2L_0$
  - 2029-2040: $\sqrt{s} = 14$ TeV (?)
    - $L = 5L_0 - 7.5L_0$

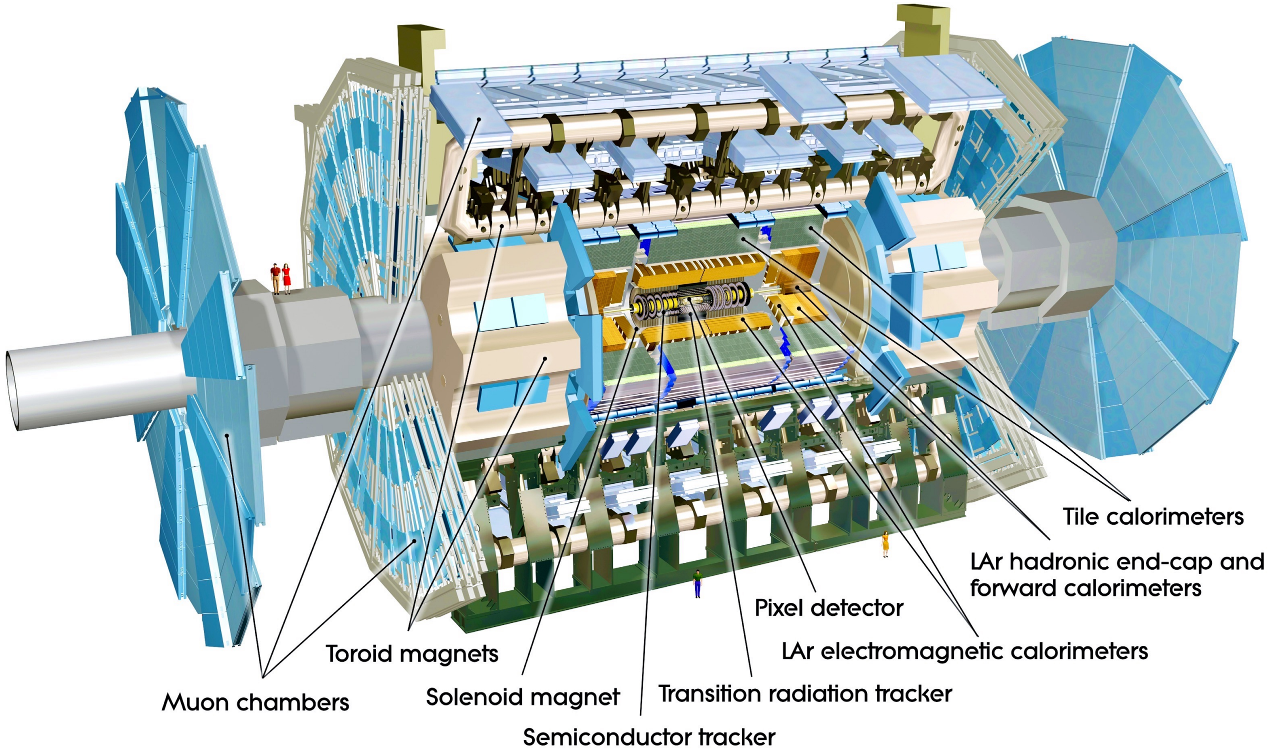

- ATLAS reference frame
  - Rapidity:

$$y = 1/2\ln[(E+p_z)/(E-p_z)]$$

  - Pseudo-rapidity:

$$\eta = -\ln\tan(\theta/2)$$

    - Where, θ is the polar angle of the experiment

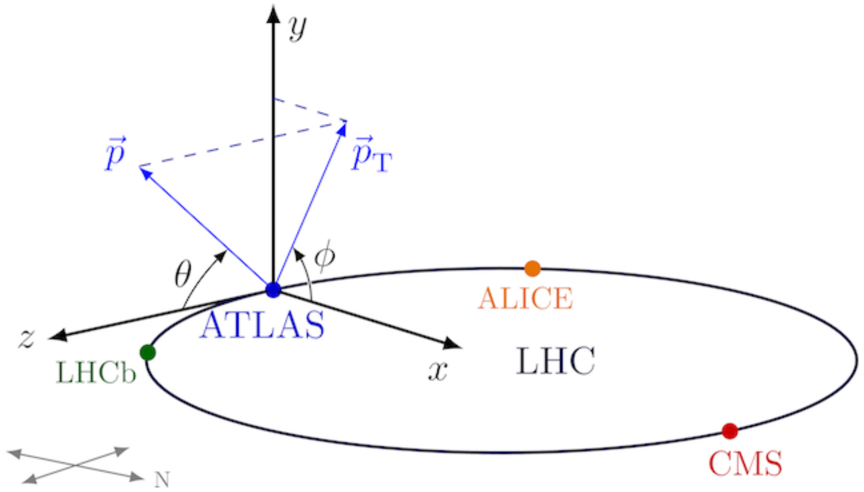

Discriminator Variables in VBS Measurements

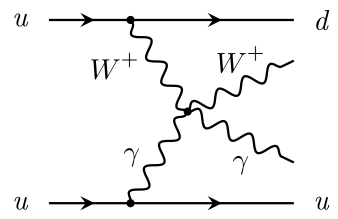

- VBS event topology
  - Two jets with leading transverse momenta in the forward regions
    - Large rapidity gap Δy_{jj} (Lorentz invariant!)
    - Large invariant mass m_{jj}
  - Vector bosons in a central region
  - No additional jet activity in the gap region
    - $N_{gapjets}$

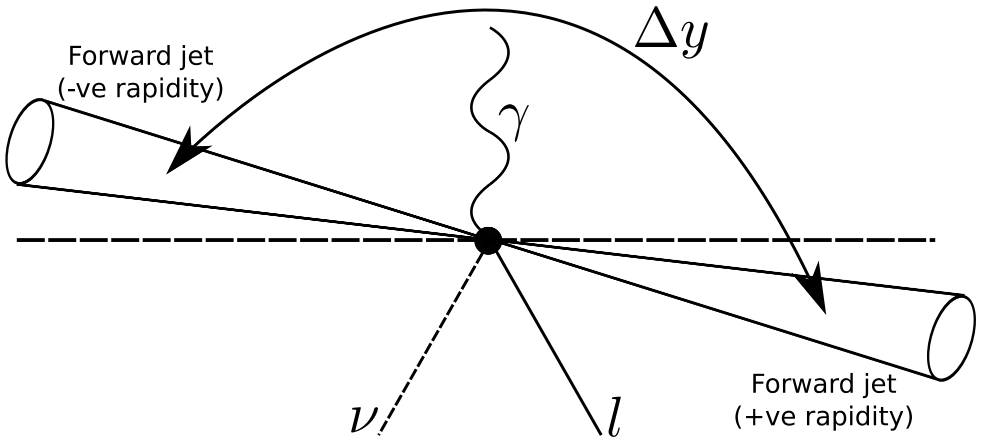

- Invariant mass of leading jets: $m_{jj} = \sqrt{(p_{j1} + p_{j2})^2}$

- Lepton-photon centrality: $\xi_{l+\gamma} = \left| y_{l+\gamma} - \frac{y_{j1}+y_{j2}}{2} \right| / |\Delta y_{jj}|$
  - Can be also defined for other objects or combinations of objects

Same Sign $W^{\pm}W^{\pm}jj$ Measurement

arXiv:2312.00420

$\sqrt{s} = 13\,TeV,\ 139\,fb^{-1}$

- $W^{\pm}W^{\pm}jj$ has the largest ratio of the electroweak to QCD production cross sections among all vector boson scattering (VBS) sensitive $VVjj$ final states
  - As the QCD leading order diagrams with initial gluons are forbidden

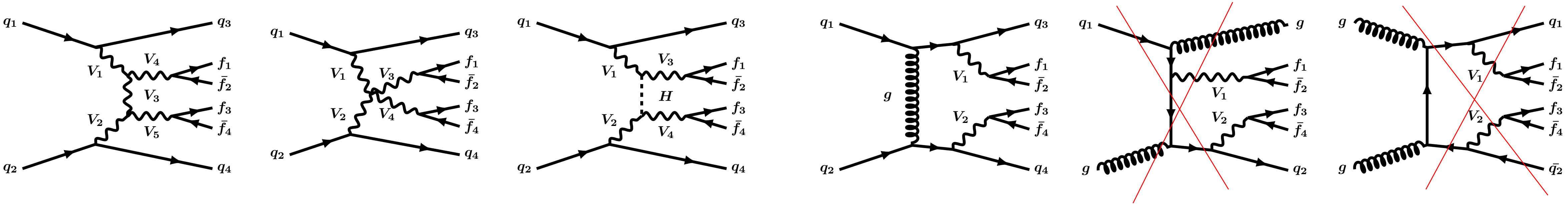

Same Sign $W^{\pm}W^{\pm}jj$ Measurement

arXiv:2312.00420

$\sqrt{s} = 13\,TeV,\ 139\,fb^{-1}$

- ❑ $W^{\pm}W^{\pm}jj$ has the largest ratio of the electroweak to QCD production cross sections among all vector boson scattering (VBS) sensitive $VVjj$ final states
  - ❖ As the QCD leading order diagrams with initial gluons are forbidden

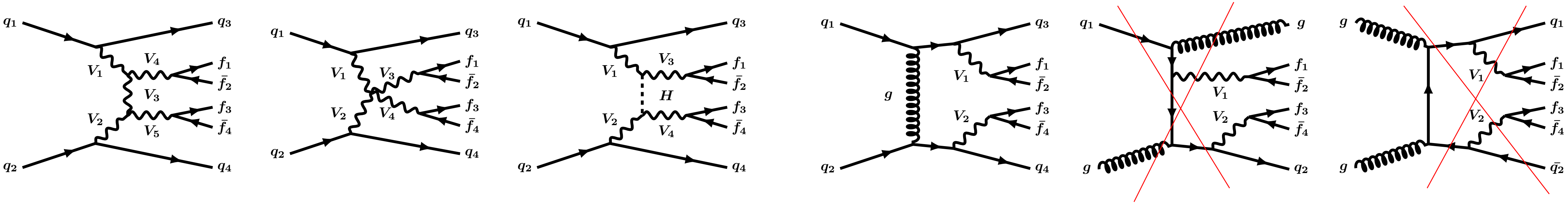

- ❑ Data, signal and background pre-fit event yields in the Signal Region
  - ✦ 2 sub-regions for electron-muon pairs distinguished by the leading-p_T lepton flavour

Process	ee	$e\mu$	μe	$\mu\mu$	Combined
$W^{\pm}W^{\pm}jj$ EW	27.6 ± 0.9	68.2 ± 1.6	61.3 ± 1.5	77.8 ± 1.7	235 ± 5
$W^{\pm}W^{\pm}jj$ QCD	1.6 ± 0.5	7.3 ± 2.2	6.4 ± 1.9	8.8 ± 2.5	24 ± 7
$W^{\pm}W^{\pm}jj$ Int	0.93 ± 0.20	2.2 ± 0.5	2.0 ± 0.4	2.5 ± 0.5	7.6 ± 1.6
$W^{\pm}Zjj$ QCD	8.4 ± 1.0	26.8 ± 3.0	26.7 ± 3.0	20.9 ± 2.2	83 ± 9
$W^{\pm}Zjj$ EW	1.71 ± 0.14	4.9 ± 0.4	4.1 ± 0.4	4.2 ± 0.4	14.9 ± 1.2
Non-prompt	8.9 ± 2.6	15 ± 4	10.2 ± 3.2	21 ± 7	56 ± 12
$V\gamma$	1.3 ± 0.8	5.1 ± 2.2	4.6 ± 2.6	—	11 ± 5
Charge misid.	3.8 ± 2.0	5.0 ± 1.3	1.2 ± 0.4	—	10 ± 4
Other prompt	1.02 ± 0.29	2.5 ± 0.6	1.8 ± 0.5	1.7 ± 2.2	7.1 ± 2.8
Total expected	55 ± 4	137 ± 7	118 ± 6	137 ± 8	448 ± 20
Data	52	149	127	147	475

- ❑ EW signal purity of 52% vs. 5.4% of QCD background

Same Sign $\boldsymbol{W^{\pm}W^{\pm}jj}$ Measurement

- Fiducial cross section = MC fiducial cross section × fitted singal normalisation

- The signal and the main QCD $WZjj$ background normalisations obtained from the simultaneous profile-likelihood fit to the m_{jj} distributions in the signal region, the low-m_{jj} control region and the integrated (single bin) QCD $WZjj$ control region

Same Sign $W^{\pm}W^{\pm}jj$ Measurement

- Fiducial cross section = MC fiducial cross section × fitted singal normalisation

- The signal and the main QCD $WZjj$ background normalisations obtained from the simultaneous profile-likelihood fit to the m_{jj} distributions in the signal region, the low-m_{jj} control region and the integrated (single bin) QCD $WZjj$ control region

Description	$\sigma_{\text{fid}}^{\text{EW}}$ [fb]	$\sigma_{\text{fid}}^{\text{EW+Int+QCD}}$ [fb]
Measured cross section	$2.92 \pm 0.22\,(\text{stat.}) \pm 0.19\,(\text{syst.})$	$3.38 \pm 0.22\,(\text{stat.}) \pm 0.19\,(\text{syst.})$
MG5_aMC+Herwig7	$2.53 \pm 0.04\,(\text{PDF})\,^{+0.22}_{-0.19}\,(\text{scale})$	$2.92 \pm 0.05\,(\text{PDF})\,^{+0.34}_{-0.27}\,(\text{scale})$
MG5_aMC+Pythia8	$2.53 \pm 0.04\,(\text{PDF})\,^{+0.22}_{-0.19}\,(\text{scale})$	$2.90 \pm 0.05\,(\text{PDF})\,^{+0.33}_{-0.26}\,(\text{scale})$
Sherpa	$2.48 \pm 0.04\,(\text{PDF})\,^{+0.40}_{-0.27}\,(\text{scale})$	$2.92 \pm 0.03\,(\text{PDF})\,^{+0.60}_{-0.40}\,(\text{scale})$
Sherpa ⊗ NLO EW	$2.10 \pm 0.03\,(\text{PDF})\,^{+0.34}_{-0.23}\,(\text{scale})$	$2.54 \pm 0.03\,(\text{PDF})\,^{+0.50}_{-0.33}\,(\text{scale})$
Powheg Box+Pythia	2.64	–

- Good agreement found for the fiducial cross sections with the SM predictions within the measurement uncertainties
  - ✦ Total uncertainty: 9.8% (data statistical: 7.4%, instrumental and theoretical: 6.4%)

Same Sign $W^{\pm}W^{\pm}jj$ Measurement

- Differential cross sections obtained using the profile-likelihood unfolding method

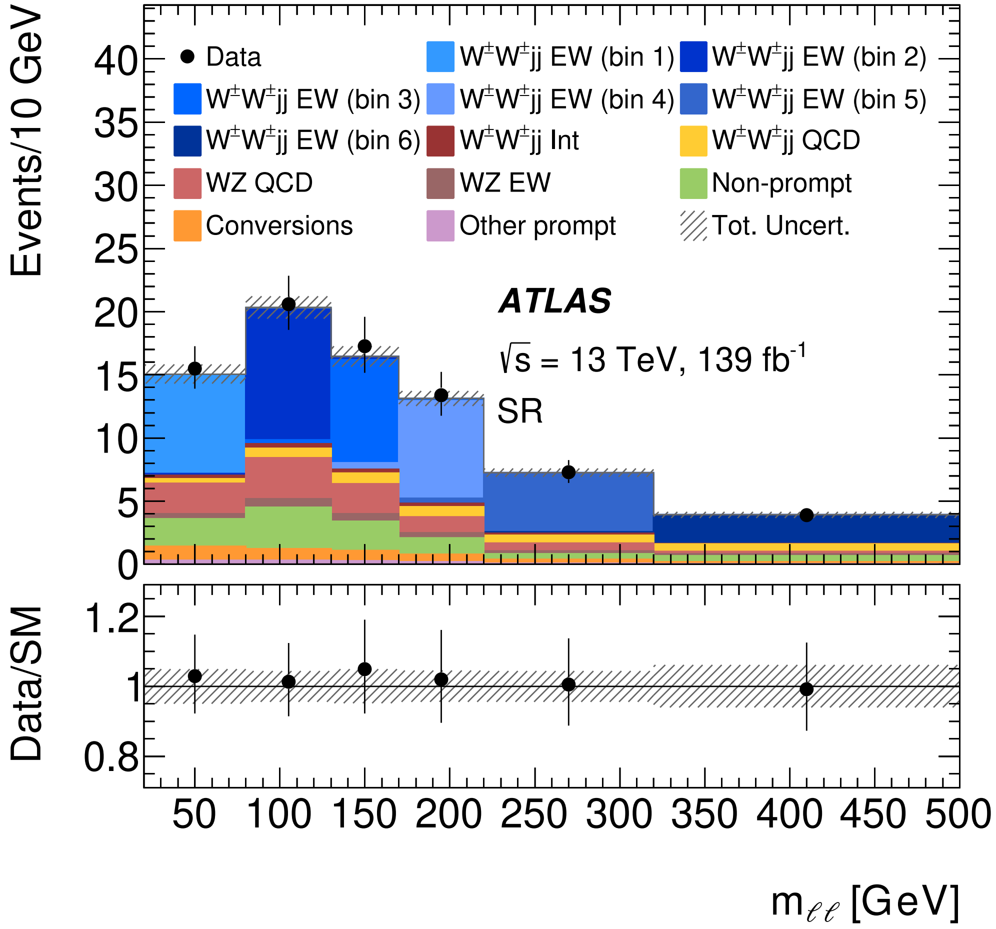

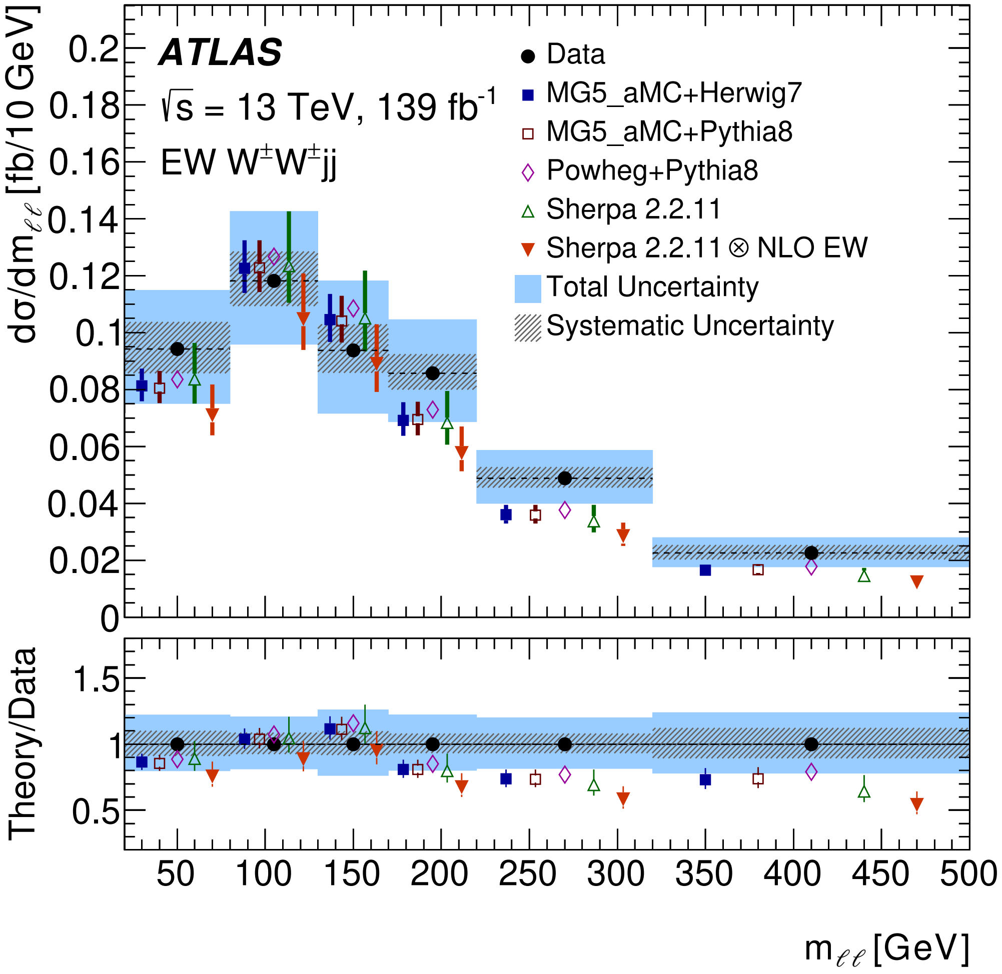

Same Sign $W^{\pm}W^{\pm}jj$ Measurement

- Simulated and reconstructed EFT samples are fitted to the detector-level m_{ll} distributions in the SR and CRs to obtain limits on a corresponding c_i (or c_i and c_j in case of two-dimensional limits) that is a free parameter of the fit
  - Only one c_i (or c_i and c_j pair) is taken as non-zero at a time
  - Nominal predictions for the SM signal and backgrounds are assumed

$$|A_{\rm SM}|^2 + \sum_i c_i 2Re(A^*_{\rm SM}A_i) + \sum_i c_i{}^2|A_i|^2 + \sum_{ij,i\neq j} c_i c_j 2Re(A_i A^*_j)$$

Same Sign $W^{\pm}W^{\pm}jj$ Measurement

- Simulated and reconstructed EFT samples are fitted to the detector-level m_{ll} distributions in the SR and CRs to obtain limits on a corresponding c_i (or c_i and c_j in case of two-dimensional limits) that is a free parameter of the fit
  - Only one c_i (or c_i and c_j pair) is taken as non-zero at a time
  - Nominal predictions for the SM signal and backgrounds are assumed

- EFT samples are simulated without and with different cut-off scales applied to the invariant mass of the final state di-boson system, $\boldsymbol{m_{WV}}$, in every event at the truth particle level

$$|A_{\mathrm{SM}}|^2 + \sum_i c_i 2Re(A_{\mathrm{SM}}^* A_i) + \sum_i {c_i}^2 |A_i|^2 + \sum_{ij,i\neq j} c_i c_j 2Re(A_i A_j^*)$$

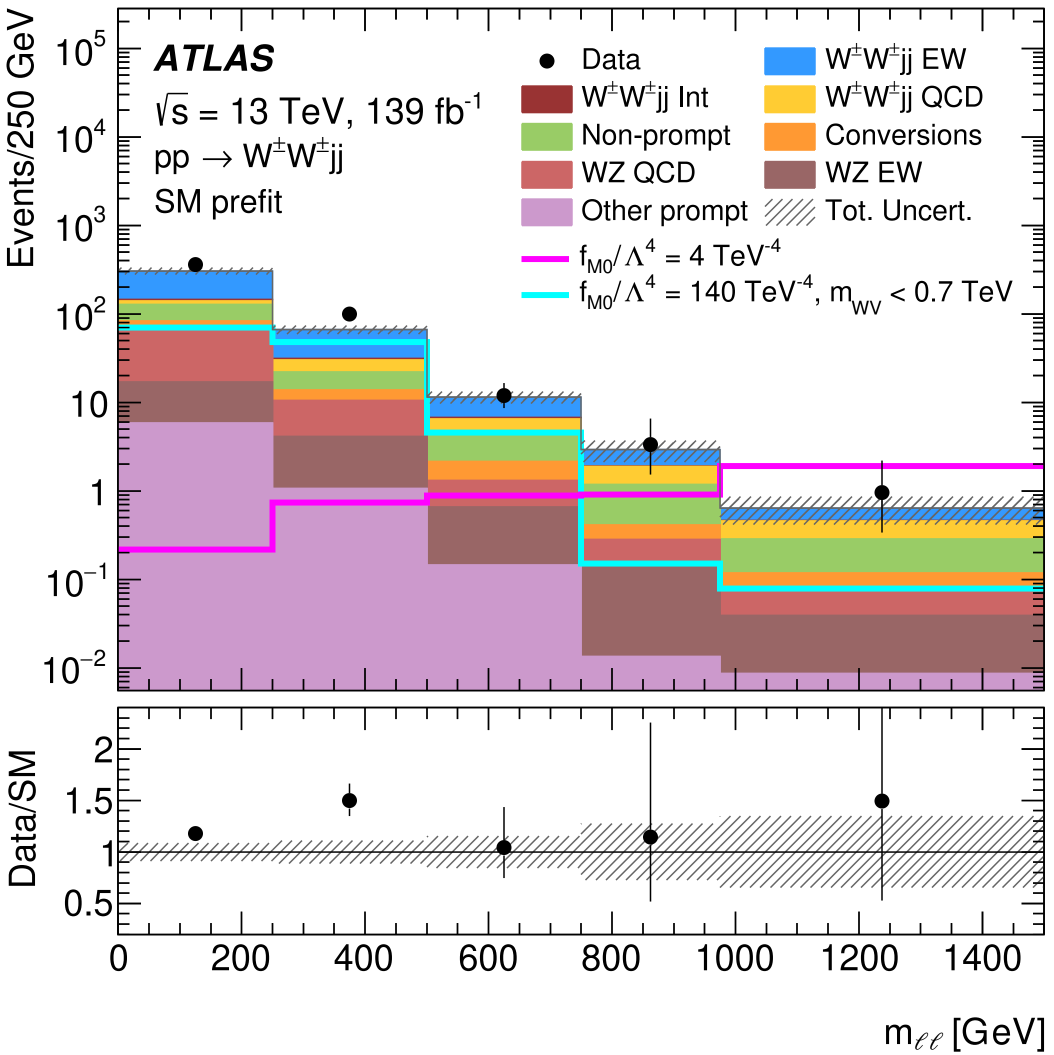

Same Sign $W^{\pm}W^{\pm}jj$ Measurement

- ❑ **Competitive limits** (@ 95% C.L.) are set on the coefficients of the relevant EFT dimension-8 operators that have large effects on the $WWWW$ coupling

	WWWW	WWZZ	ZZZZ	WWAZ	WWAA	ZZZA	ZZAA	ZAAA	AAAA
$\mathcal{O}_{S,0}$, $\mathcal{O}_{S,1}$	X	X	X						
$\mathcal{O}_{M,0}$, $\mathcal{O}_{M,1}$,$\mathcal{O}_{M,6}$,$\mathcal{O}_{M,7}$	X	X	X	X	X	X	X		
$\mathcal{O}_{M,2}$,$\mathcal{O}_{M,3}$, $\mathcal{O}_{M,4}$,$\mathcal{O}_{M,5}$		X	X	X	X	X	X		
$\mathcal{O}_{T,0}$,$\mathcal{O}_{T,1}$,$\mathcal{O}_{T,2}$	X	X	X	X	X	X	X	X	X
$\mathcal{O}_{T,5}$,$\mathcal{O}_{T,6}$,$\mathcal{O}_{T,7}$		X	X	X	X	X	X	X	X
$\mathcal{O}_{T,8}$,$\mathcal{O}_{T,9}$			X			X	X	X	X

TABLE II: Quartic vertices modified by each dimension-8 operator are marked with X.

Same Sign $W^{\pm}W^{\pm}jj$ Measurement

- **Competitive limits** (@ 95% C.L.) are set on the coefficients of the relevant EFT dimension-8 operators that have large effects on the $WWWW$ coupling

	WWWW	WWZZ	ZZZZ	WWAZ	WWAA	ZZZA	ZZAA	ZAAA	AAAA
$\mathcal{O}_{S,0}$, $\mathcal{O}_{S,1}$	X	X	X						
$\mathcal{O}_{M,0}$, $\mathcal{O}_{M,1}$, $\mathcal{O}_{M,6}$, $\mathcal{O}_{M,7}$	X	X	X	X	X	X	X		
$\mathcal{O}_{M,2}$, $\mathcal{O}_{M,3}$, $\mathcal{O}_{M,4}$, $\mathcal{O}_{M,5}$		X	X	X	X	X	X		
$\mathcal{O}_{T,0}$, $\mathcal{O}_{T,1}$, $\mathcal{O}_{T,2}$	X	X	X	X	X	X	X	X	X
$\mathcal{O}_{T,5}$, $\mathcal{O}_{T,6}$, $\mathcal{O}_{T,7}$		X	X	X	X	X	X	X	X
$\mathcal{O}_{T,8}$, $\mathcal{O}_{T,9}$			X			X	X	X	X

TABLE II: Quartic vertices modified by each dimension-8 operator are marked with X.

Coefficient	Type	No unitarisation cut-off [TeV^{-4}]	Lower, upper limit at the respective unitarity bound [TeV^{-4}]
$f_{\mathrm{M0}}/\Lambda^4$	Exp.	[-3.9, 3.8]	-64 at 0.9 TeV, 40 at 1.0 TeV
	Obs.	[-4.1, 4.1]	-140 at 0.7 TeV, 117 at 0.8 TeV
$f_{\mathrm{M1}}/\Lambda^4$	Exp.	[-6.3, 6.6]	-25.5 at 1.6 TeV, 31 at 1.5 TeV
	Obs.	[-6.8, 7.0]	-45 at 1.4 TeV, 54 at 1.3 TeV
$f_{\mathrm{M7}}/\Lambda^4$	Exp.	[-9.3, 8.8]	-33 at 1.8 TeV, 29.1 at 1.8 TeV
	Obs.	[-9.8, 9.5]	-39 at 1.7 TeV, 42 at 1.7 TeV
$f_{\mathrm{S02}}/\Lambda^4$	Exp.	[-5.5, 5.7]	-94 at 0.8 TeV, 122 at 0.7 TeV
	Obs.	[-5.9, 5.9]	–
$f_{\mathrm{S1}}/\Lambda^4$	Exp.	[-22.0, 22.5]	–
	Obs.	[-23.5, 23.6]	–
$f_{\mathrm{T0}}/\Lambda^4$	Exp.	[-0.34, 0.34]	-3.2 at 1.2 TeV, 4.9 at 1.1 TeV
	Obs.	[-0.36, 0.36]	-7.4 at 1.0 TeV, 12.4 at 0.9 TeV
$f_{\mathrm{T1}}/\Lambda^4$	Exp.	[-0.158, 0.174]	-0.32 at 2.6 TeV, 0.44 at 2.4 TeV
	Obs.	[-0.174, 0.186]	-0.38 at 2.5 TeV, 0.49 at 2.4 TeV
$f_{\mathrm{T2}}/\Lambda^4$	Exp.	[-0.56, 0.70]	-2.60 at 1.7 TeV, 10.3 at 1.2 TeV
	Obs.	[-0.63, 0.74]	–

Same Sign $W^{\pm}W^{\pm}jj$ Measurement

- **Competitive limits** (@ 95% C.L.) are set on the coefficients of the relevant EFT dimension-8 operators that have large effects on the $WWWW$ coupling

	WWWW	WWZZ	ZZZZ	WWAZ	WWAA	ZZZA	ZZAA	ZAAA	AAAA
$\mathcal{O}_{S,0}$, $\mathcal{O}_{S,1}$	X	X	X						
$\mathcal{O}_{M,0}$, $\mathcal{O}_{M,1}$,$\mathcal{O}_{M,6}$,$\mathcal{O}_{M,7}$	X	X	X	X	X	X	X		
$\mathcal{O}_{M,2}$,$\mathcal{O}_{M,3}$, $\mathcal{O}_{M,4}$,$\mathcal{O}_{M,5}$		X	X	X	X	X	X		
$\mathcal{O}_{T,0}$,$\mathcal{O}_{T,1}$,$\mathcal{O}_{T,2}$	X	X	X	X	X	X	X	X	X
$\mathcal{O}_{T,5}$,$\mathcal{O}_{T,6}$,$\mathcal{O}_{T,7}$		X	X	X	X	X	X	X	X
$\mathcal{O}_{T,8}$,$\mathcal{O}_{T,9}$			X			X	X	X	X

TABLE II: Quartic vertices modified by each dimension-8 operator are marked with X.

Coefficient	Type	No unitarisation cut-off [TeV^{-4}]	Lower, upper limit at the respective unitarity bound [TeV^{-4}]
f_{M0}/Λ^4	Exp.	[-3.9, 3.8]	-64 at 0.9 TeV, 40 at 1.0 TeV
	Obs.	[-4.1, 4.1]	-140 at 0.7 TeV, 117 at 0.8 TeV
f_{M1}/Λ^4	Exp.	[-6.3, 6.6]	-25.5 at 1.6 TeV, 31 at 1.5 TeV
	Obs.	[-6.8, 7.0]	-45 at 1.4 TeV, 54 at 1.3 TeV
f_{M7}/Λ^4	Exp.	[-9.3, 8.8]	-33 at 1.8 TeV, 29.1 at 1.8 TeV
	Obs.	[-9.8, 9.5]	-39 at 1.7 TeV, 42 at 1.7 TeV
f_{S02}/Λ^4	Exp.	[-5.5, 5.7]	-94 at 0.8 TeV, 122 at 0.7 TeV
	Obs.	[-5.9, 5.9]	–
f_{S1}/Λ^4	Exp.	[-22.0, 22.5]	–
	Obs.	[-23.5, 23.6]	–
f_{T0}/Λ^4	Exp.	[-0.34, 0.34]	-3.2 at 1.2 TeV, 4.9 at 1.1 TeV
	Obs.	[-0.36, 0.36]	-7.4 at 1.0 TeV, 12.4 at 0.9 TeV
f_{T1}/Λ^4	Exp.	[-0.158, 0.174]	-0.32 at 2.6 TeV, 0.44 at 2.4 TeV
	Obs.	[-0.174, 0.186]	-0.38 at 2.5 TeV, 0.49 at 2.4 TeV
f_{T2}/Λ^4	Exp.	[-0.56, 0.70]	-2.60 at 1.7 TeV, 10.3 at 1.2 TeV
	Obs.	[-0.63, 0.74]	–

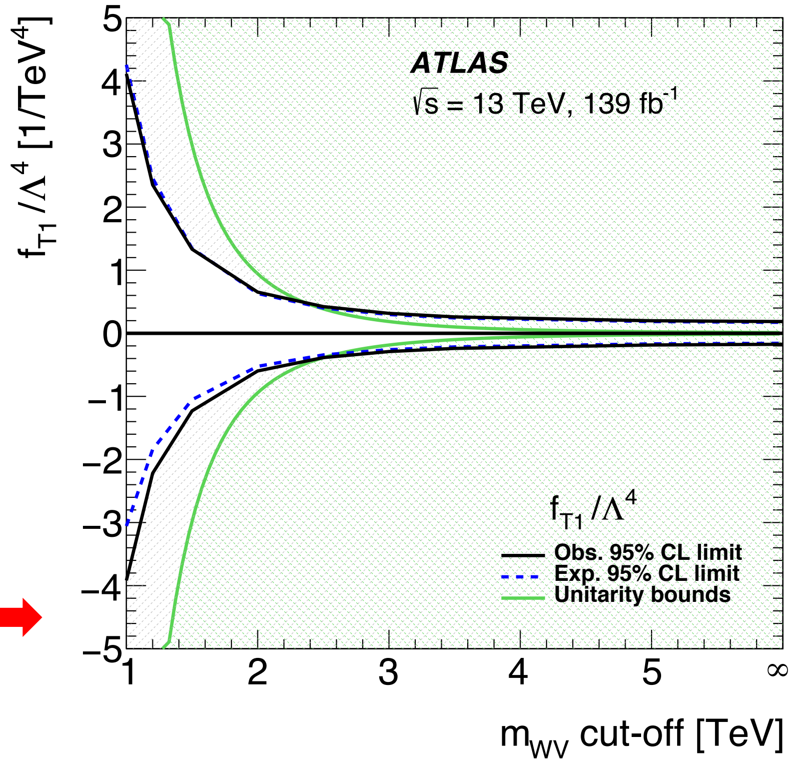

$ZZ(\rightarrow 4l)jj$ Differential Cross Sections

JHEP 01 (2024) 004

$\sqrt{s} = 13\,TeV,\ 140\,fb^{-1}$

- Differential cross sections are measured in VBS-enhanced ($\zeta < 0.4$) and VBS-suppressed ($\zeta > 0.4$) regions
  - Three types of observables are measured
    - **VBS observables**
    - Polarisation, charge conjugation and parity observables
    - QCD-sensitive observables
  - Both EW and QCD production mechanisms are probed

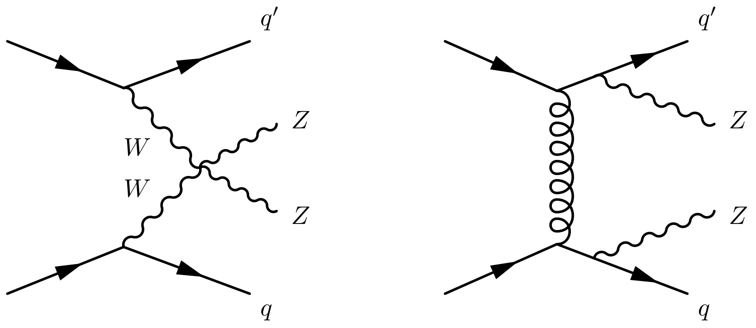

$$\zeta = \left| \frac{\left[y_{4\ell} - 0.5(y_{j_1} + y_{j_2})\right]}{\Delta y_{jj}} \right|$$

$ZZ(\rightarrow 4l)jj$ Differential Cross Sections

JHEP 01 (2024) 004

$\sqrt{s} = 13\,TeV,\ 140\,fb^{-1}$

- Differential cross sections are measured in VBS-enhanced ($\zeta < 0.4$) and VBS-suppressed ($\zeta > 0.4$) regions
  - Three types of observables are measured
    - **VBS observables**
    - Polarisation, charge conjugation and parity observables
    - QCD-sensitive observables
  - Both EW and QCD production mechanisms are probed

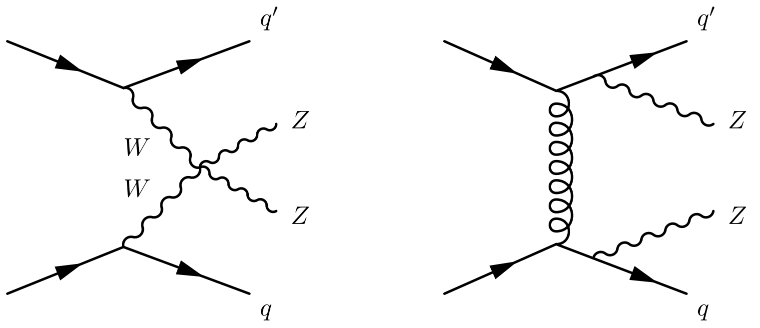

$$\zeta = \left| \frac{\left[y_{4\ell} - 0.5(y_{j_1} + y_{j_2})\right]}{\Delta y_{jj}} \right|$$

- Two Z bosons are selected from the same-flavour opposite-charge lepton pairs
  - Have smallest $|m_{ll} - m_Z|$
  - Are formed from different leptons

Process	Event yield ± stat. ± syst.	
	VBS-enhanced	VBS-suppressed
strong $4\ell jj$ (Sherpa)	98.9 ± 0.5 ± 25.2	45.5 ± 0.3 ± 12.9
EW $4\ell jj$ (MG5+Py8)	24.1 ± 0.1 ± 1.8	2.12 ± 0.02 ± 0.14
Prompt background	18.8 ± 0.2 ± 2.2	5.5 ± 0.1 ± 0.4
Non-prompt background	3.0 ± 0.6 ± 3.2	1.1 ± 0.5 ± 1.2
Total prediction	144 ± 1 ± 26	54 ± 1 ± 13
Data	169	53

$ZZ(\rightarrow 4l)jj$ Differential Cross Sections

- Event distributions of the invariant masses of four leptons (left) and two leading jets (right) in the VBS-enhanced signal region

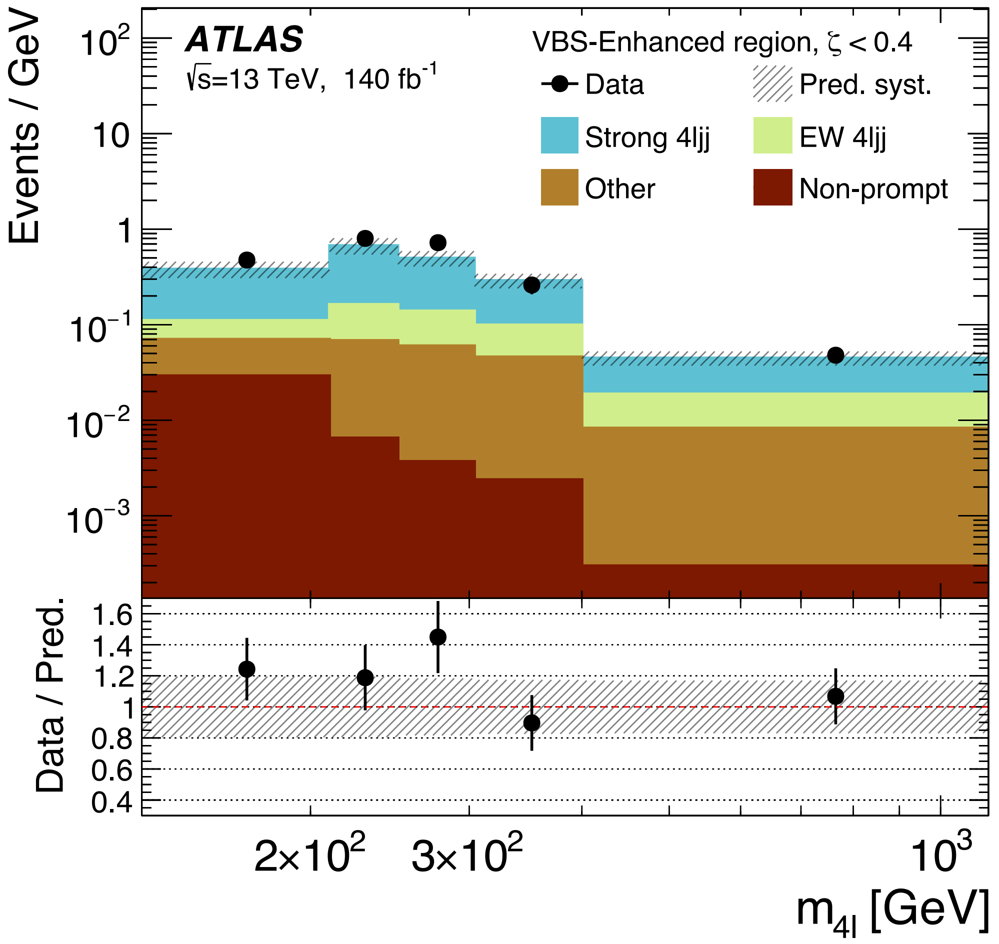

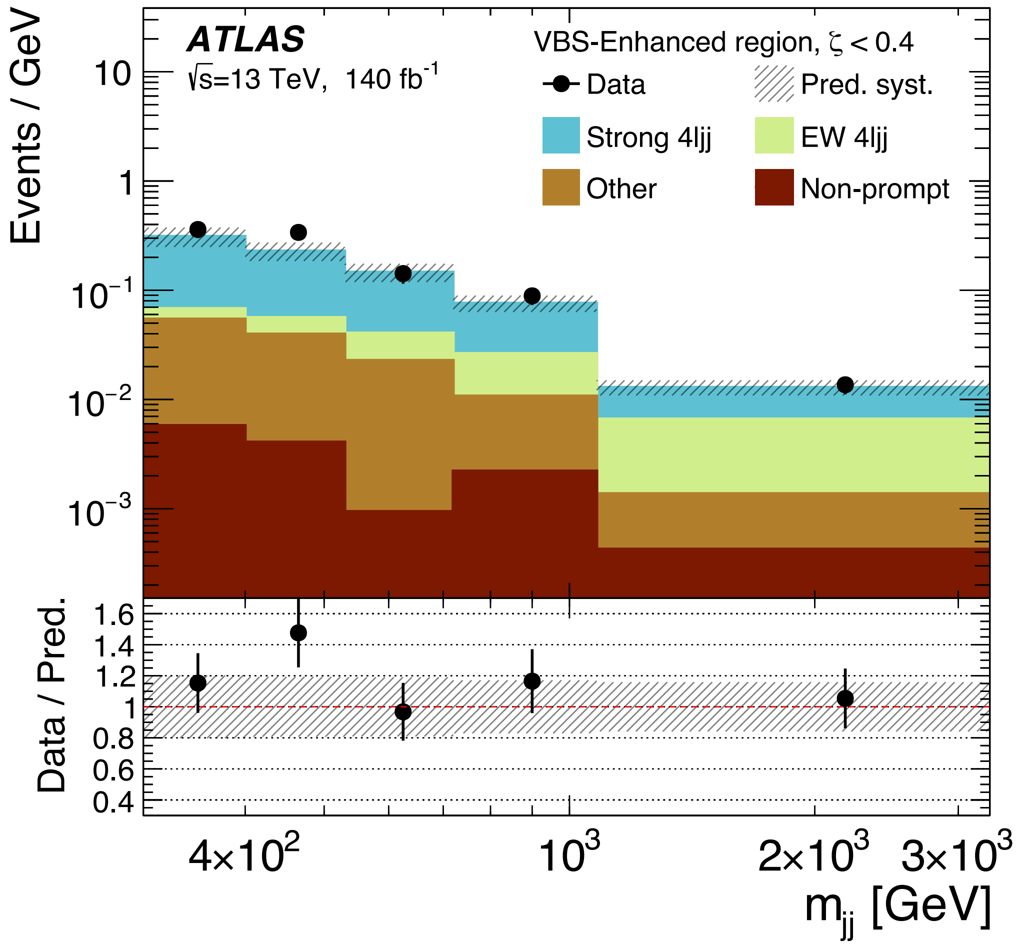

$ZZ(\rightarrow 4l)jj$ Differential Cross Sections

- Iterative Bayesian unfolding is used to measure differential cross sections

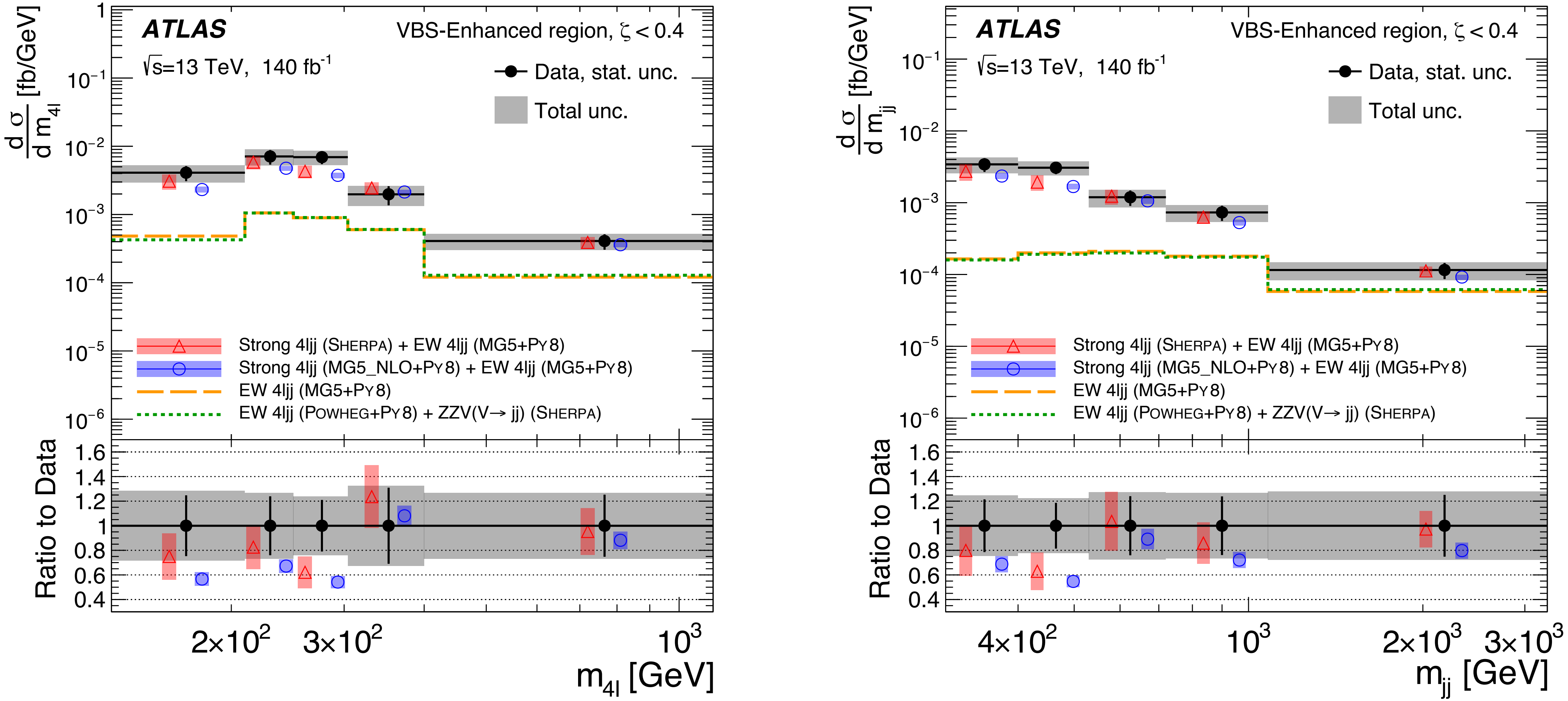

$ZZ(\rightarrow 4l)jj$ Differential Cross Sections

- EFT samples combined with the SM signal are fitted simultaneously to the unfolded m_{4l} and m_{jj} distributions and limits (@ 95% C.L.) on anomalous couplings of dimension-8 operators are obtained

$$\boxed{\mathcal{L} = \mathcal{L}_{\mathrm{SM}} + \sum_i \frac{f_{\mathrm{T},i}}{\Lambda^4} \mathcal{O}_{\mathrm{T},i}}$$

	WWWW	WWZZ	ZZZZ	WWAZ	WWAA	ZZZA	ZZAA	ZAAA	AAAA
$\mathcal{O}_{S,0}$, $\mathcal{O}_{S,1}$	X	X	X						
$\mathcal{O}_{M,0}$, $\mathcal{O}_{M,1}$, $\mathcal{O}_{M,6}$, $\mathcal{O}_{M,7}$	X	X	X	X	X	X	X		
$\mathcal{O}_{M,2}$, $\mathcal{O}_{M,3}$, $\mathcal{O}_{M,4}$, $\mathcal{O}_{M,5}$		X	X	X	X	X	X		
$\mathcal{O}_{T,0}$, $\mathcal{O}_{T,1}$, $\mathcal{O}_{T,2}$	X	X	X	X	X	X	X	X	X
$\mathcal{O}_{T,5}$, $\mathcal{O}_{T,6}$, $\mathcal{O}_{T,7}$		X	X	X	X	X	X	X	X
$\mathcal{O}_{T,8}$, $\mathcal{O}_{T,9}$			X			X	X	X	X

TABLE II: Quartic vertices modified by each dimension-8 operator are marked with X.

$ZZ(\rightarrow 4l)jj$ Differential Cross Sections

- EFT samples combined with the SM signal are fitted simultaneously to the unfolded m_{4l} and m_{jj} distributions and limits (@ 95% C.L.) on anomalous couplings of dimension-8 operators are obtained

	WWWW	WWZZ	ZZZZ	WWAZ	WWAA	ZZZA	ZZAA	ZAAA	AAAA
$\mathcal{O}_{S,0}$, $\mathcal{O}_{S,1}$	X	X	X						
$\mathcal{O}_{M,0}$, $\mathcal{O}_{M,1}$, $\mathcal{O}_{M,6}$, $\mathcal{O}_{M,7}$	X	X	X	X	X	X	X		
$\mathcal{O}_{M,2}$, $\mathcal{O}_{M,3}$, $\mathcal{O}_{M,4}$, $\mathcal{O}_{M,5}$		X	X	X	X	X	X		
$\mathcal{O}_{T,0}$, $\mathcal{O}_{T,1}$, $\mathcal{O}_{T,2}$	X	X	X	X	X	X	X	X	X
$\mathcal{O}_{T,5}$, $\mathcal{O}_{T,6}$, $\mathcal{O}_{T,7}$		X	X	X	X	X	X	X	X
$\mathcal{O}_{T,8}$, $\mathcal{O}_{T,9}$			X			X	X	X	X

TABLE II: Quartic vertices modified by each dimension-8 operator are marked with X.

$$\mathcal{L} = \mathcal{L}_{\mathrm{SM}} + \sum_i \frac{f_{\mathrm{T},i}}{\Lambda^4} O_{\mathrm{T},i}$$

Wilson coefficient	$\lvert\mathcal{M}_{d8}\rvert^2$ Included	95% confidence interval [TeV^{-4}] Expected	Observed
$f_{\mathrm{T},0}/\Lambda^4$	yes	[-0.98, 0.93]	[-1.00, 0.97]
	no	[-23, 17]	[-19, 19]
$f_{\mathrm{T},1}/\Lambda^4$	yes	[-1.2, 1.2]	[-1.3, 1.3]
	no	[-160, 120]	[-140, 140]
$f_{\mathrm{T},2}/\Lambda^4$	yes	[-2.5, 2.4]	[-2.6, 2.5]
	no	[-74, 56]	[-63, 62]
$f_{\mathrm{T},5}/\Lambda^4$	yes	[-2.5, 2.4]	[-2.6, 2.5]
	no	[-79, 60]	[-68, 67]
$f_{\mathrm{T},6}/\Lambda^4$	yes	[-3.9, 3.9]	[-4.1, 4.1]
	no	[-64, 48]	[-55, 54]
$f_{\mathrm{T},7}/\Lambda^4$	yes	[-8.5, 8.1]	[-8.8, 8.4]
	no	[-260, 200]	[-220, 220]
$f_{\mathrm{T},8}/\Lambda^4$	yes	[-2.1, 2.1]	[-2.2, 2.2]
	no	[-4.6, 3.1]$\times10^4$	[-3.9, 3.8]$\times10^4$
$f_{\mathrm{T},9}/\Lambda^4$	yes	[-4.5, 4.5]	[-4.7, 4.7]
	no	[-7.5, 5.5]$\times10^4$	[-6.4, 6.3]$\times10^4$

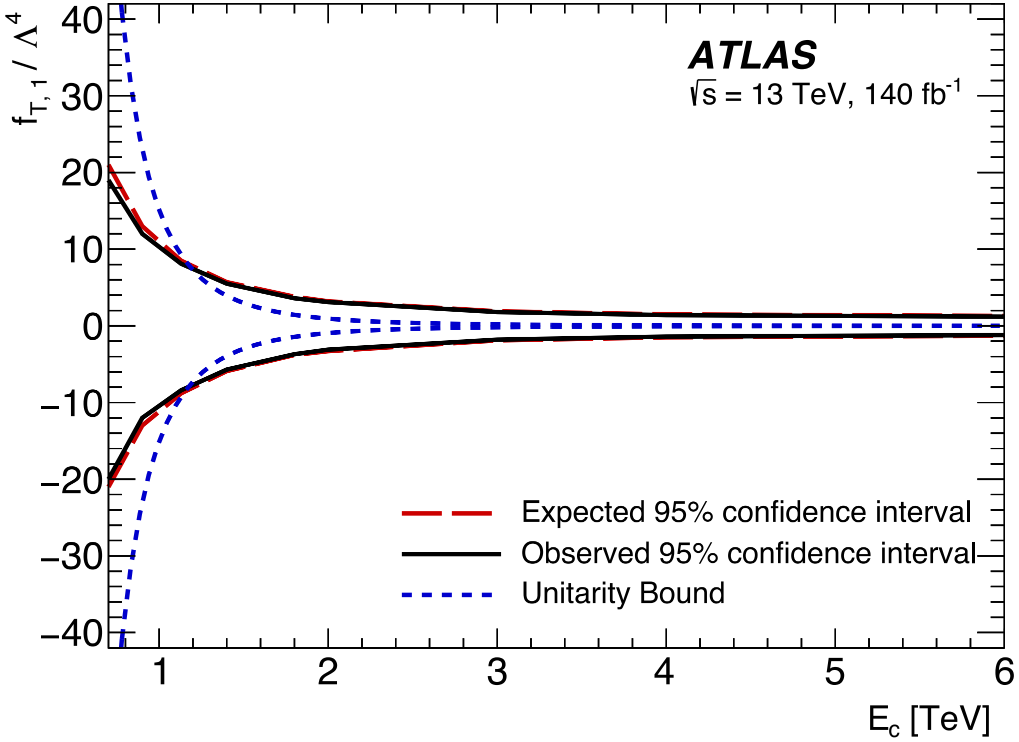

$ZZ(\to 4l)jj$ Differential Cross Sections

- EFT samples combined with the SM signal are fitted simultaneously to the unfolded m_{4l} and m_{jj} distributions and limits (@ 95% C.L.) on anomalous couplings of dimension-8 operators are obtained

	WWWW	WWZZ	ZZZZ	WWAZ	WWAA	ZZZA	ZZAA	ZAAA	AAAA
$\mathcal{O}_{S,0}$, $\mathcal{O}_{S,1}$	X	X	X						
$\mathcal{O}_{M,0}$, $\mathcal{O}_{M,1}$,$\mathcal{O}_{M,6}$,$\mathcal{O}_{M,7}$	X	X	X	X	X	X	X		
$\mathcal{O}_{M,2}$,$\mathcal{O}_{M,3}$, $\mathcal{O}_{M,4}$,$\mathcal{O}_{M,5}$		X	X	X	X	X	X		
$\mathcal{O}_{T,0}$,$\mathcal{O}_{T,1}$,$\mathcal{O}_{T,2}$	X	X	X	X	X	X	X	X	X
$\mathcal{O}_{T,5}$,$\mathcal{O}_{T,6}$,$\mathcal{O}_{T,7}$		X	X	X	X	X	X	X	X
$\mathcal{O}_{T,8}$,$\mathcal{O}_{T,9}$			X			X	X	X	X

TABLE II: Quartic vertices modified by each dimension-8 operator are marked with X.

$$\mathcal{L} = \mathcal{L}_{\mathrm{SM}} + \sum_i \frac{f_{\mathrm{T},i}}{\Lambda^4} O_{\mathrm{T},i}$$

Much stronger limits are set on these three couplings by the same sign $WWjj$ measurement (see earlier slides)

Wilson coefficient	$\lvert\mathcal{M}_{\mathrm{d8}}\rvert^2$ Included	95% confidence interval [TeV^{-4}] Expected	Observed
$f_{\mathrm{T},0}/\Lambda^4$	yes	[-0.98, 0.93]	[-1.00, 0.97]
	no	[-23, 17]	[-19, 19]
$f_{\mathrm{T},1}/\Lambda^4$	yes	[-1.2, 1.2]	[-1.3, 1.3]
	no	[-160, 120]	[-140, 140]
$f_{\mathrm{T},2}/\Lambda^4$	yes	[-2.5, 2.4]	[-2.6, 2.5]
	no	[-74, 56]	[-63, 62]
$f_{\mathrm{T},5}/\Lambda^4$	yes	[-2.5, 2.4]	[-2.6, 2.5]
	no	[-79, 60]	[-68, 67]
$f_{\mathrm{T},6}/\Lambda^4$	yes	[-3.9, 3.9]	[-4.1, 4.1]
	no	[-64, 48]	[-55, 54]
$f_{\mathrm{T},7}/\Lambda^4$	yes	[-8.5, 8.1]	[-8.8, 8.4]
	no	[-260, 200]	[-220, 220]
$f_{\mathrm{T},8}/\Lambda^4$	yes	[-2.1, 2.1]	[-2.2, 2.2]
	no	[-4.6, 3.1]$\times 10^4$	[-3.9, 3.8]$\times 10^4$
$f_{\mathrm{T},9}/\Lambda^4$	yes	[-4.5, 4.5]	[-4.7, 4.7]
	no	[-7.5, 5.5]$\times 10^4$	[-6.4, 6.3]$\times 10^4$

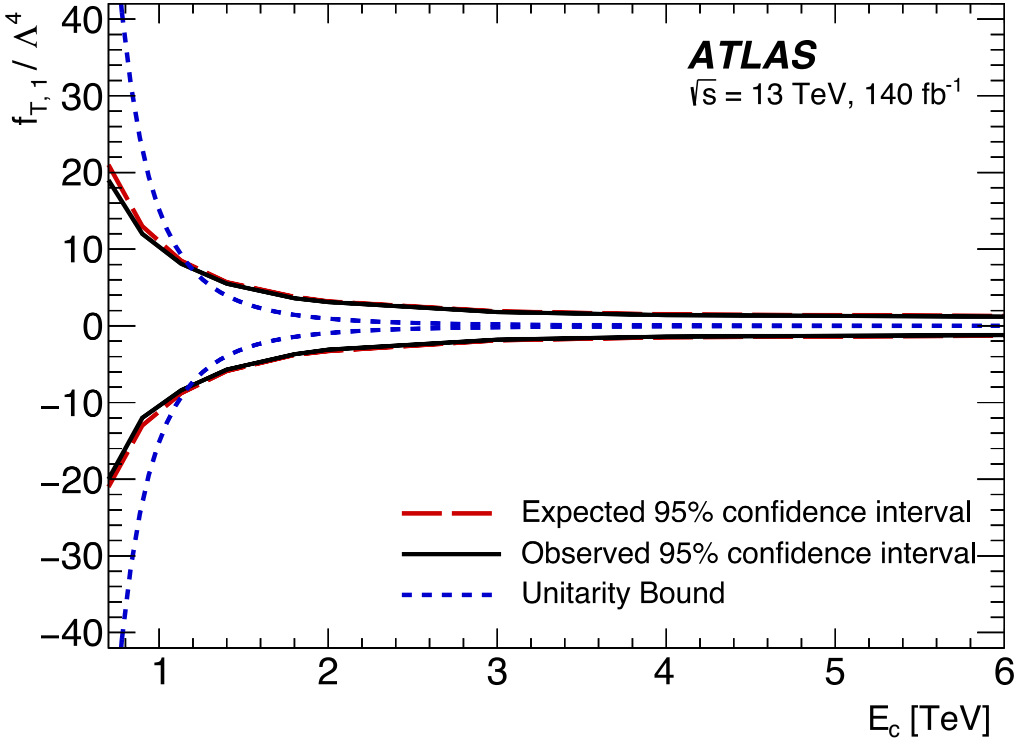

$Z(\to \nu\nu)\gamma jj$ Measurement

[JHEP06 (2023) 082](#)

$\sqrt{s} = 13\,TeV,\ 140\,fb^{-1}$

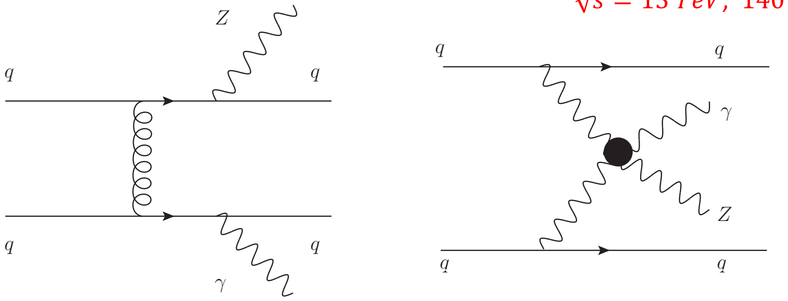

- ❑ Measurement in the high photon transverse momentum phase-space: $E_{T,\gamma} > 150$ GeV
  - ❖ Enhanced sensitivity to a possible aQGC
  - ❖ Tighter threshold values in EFT fits

$Z(\rightarrow \nu\nu)\gamma jj$ Measurement

JHEP06 (2023) 082

$\sqrt{s} = 13\,TeV,\ 140\,fb^{-1}$

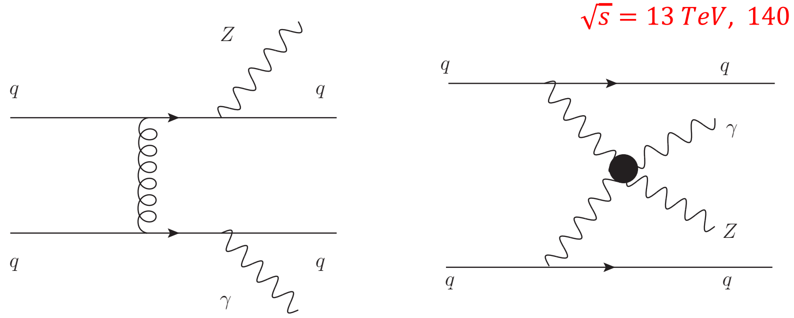

- Measurement in the high photon transverse momentum phase-space: $E_{T,\gamma} > 150$ GeV
  - Enhanced sensitivity to a possible aQGC
  - Tighter threshold values in EFT fits

- Profile-likelihood fit to the Boosted Decision Tree classifier in the SR and m_{jj} distributions in all three CRs
  - Free signal and two main background normalisations

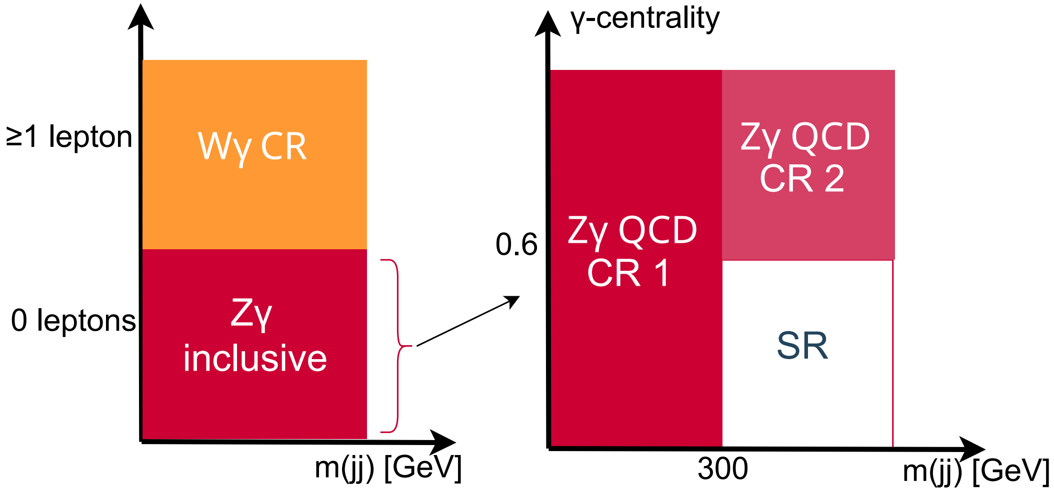

$Z(\rightarrow \nu\nu)\gamma jj$ Measurement

JHEP06 (2023) 082

$\sqrt{s} = 13\,TeV,\ 140\,fb^{-1}$

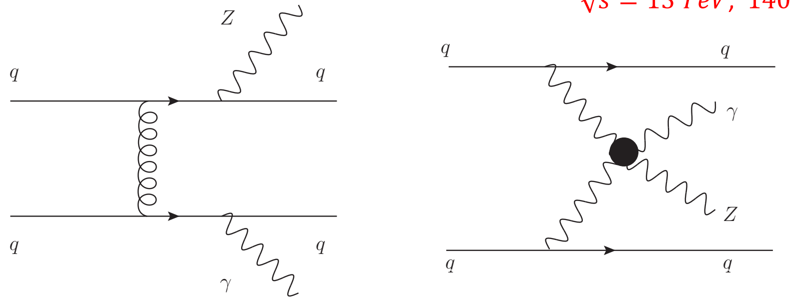

- Measurement in the high photon transverse momentum phase-space: $E_{T,\gamma} > 150$ GeV
  - Enhanced sensitivity to a possible aQGC
  - Tighter threshold values in EFT fits

- Profile-likelihood fit to the Boosted Decision Tree classifier in the SR and m_{jj} distributions in all three CRs
  - Free signal and two main background normalisations

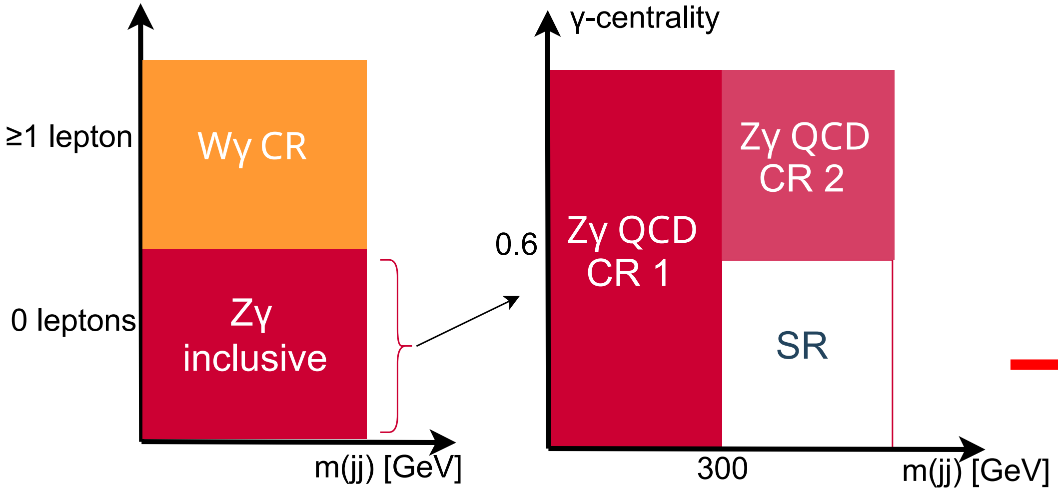

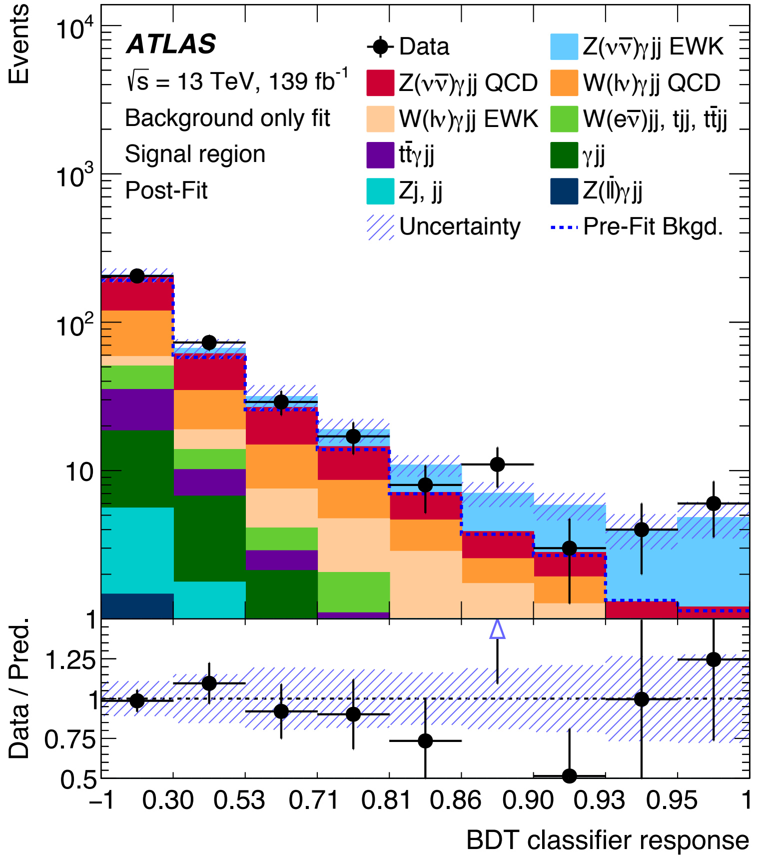

$Z(\rightarrow \nu\nu)\gamma jj$ Measurement

- Observed (expected) significance: **3.2σ (3.7σ)**
  - After combination with the ATLAS previous measurement in a low energy phase-space of $15 < E_{T,\gamma} < 115$ GeV: **6.3σ (6.6σ)**

- Predicted and measured fiducial cross sections:

$$\sigma^{\text{pred}}_{Z\gamma\text{EWK}} = 0.98 \pm 0.02\ (\text{stat.}) \pm 0.09\ (\text{scale}) \pm 0.02\ (\text{PDF})\ \text{fb}$$

$$\sigma_{Z\gamma\text{EWK}} = 0.77^{+0.34}_{-0.30}\ \text{fb} = 0.77^{+0.25}_{-0.23}\ (\text{stat.})^{+0.22}_{-0.18}\ (\text{syst.})\ \text{fb}$$

$Z(\to \nu\nu)\gamma jj$ Measurement

- Observed (expected) significance: **3.2σ (3.7σ)**
  - After combination with the ATLAS previous measurement in a low energy phase-space of $15 < E_{T,\gamma} < 115$ GeV: **6.3σ (6.6σ)**

- Predicted and measured fiducial cross sections:

$$\sigma^{\text{pred}}_{Z\gamma\text{EWK}} = 0.98 \pm 0.02\ (\text{stat.}) \pm 0.09\ (\text{scale}) \pm 0.02\ (\text{PDF})\ \text{fb}$$

$$\sigma_{Z\gamma\text{EWK}} = 0.77^{+0.34}_{-0.30}\ \text{fb} = 0.77^{+0.25}_{-0.23}\ (\text{stat.})^{+0.22}_{-0.18}\ (\text{syst.})\ \text{fb}$$

- EFT interpretation performed in the signal region
  - Adjusting (tightening) the event selection $E_{T,\gamma}$ threshold by optimisation of the expected limits for the considered dim-8 operators

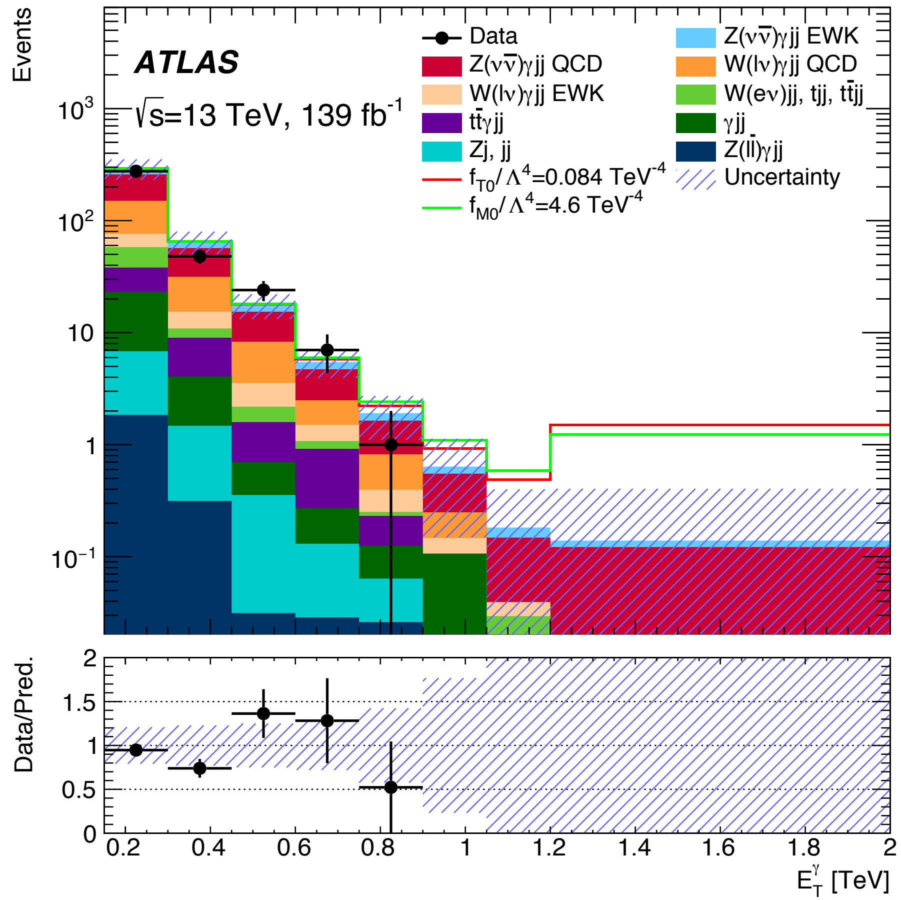

$Z(\rightarrow \nu\nu)\gamma jj$ Measurement

- **Competitive limits** (@ 95% C.L.) are obtained on the coefficients of seven relevant EFT dimension-8 operators without and with applying an energy cut-off scale to the invariant mass $m_{Z\gamma}$

	WWWW	WWZZ	ZZZZ	WWAZ	WWAA	ZZZA	ZZAA	ZAAA	AAAA
$\mathcal{O}_{S,0}$, $\mathcal{O}_{S,1}$	X	X	X						
$\mathcal{O}_{M,0}$, $\mathcal{O}_{M,1}$,$\mathcal{O}_{M,6}$,$\mathcal{O}_{M,7}$	X	X	X	X	X	X	X		
$\mathcal{O}_{M,2}$,$\mathcal{O}_{M,3}$, $\mathcal{O}_{M,4}$,$\mathcal{O}_{M,5}$		X	X	X	X	X	X		
$\mathcal{O}_{T,0}$,$\mathcal{O}_{T,1}$,$\mathcal{O}_{T,2}$	X	X	X	X	X	X	X	X	X
$\mathcal{O}_{T,5}$,$\mathcal{O}_{T,6}$,$\mathcal{O}_{T,7}$		X	X	X	X	X	X	X	X
$\mathcal{O}_{T,8}$,$\mathcal{O}_{T,9}$			X			X	X	X	X

TABLE II: Quartic vertices modified by each dimension-8 operator are marked with X.

$Z(\to \nu\nu)\gamma jj$ Measurement

- **Competitive limits** (@ 95% C.L.) are obtained on the coefficients of seven relevant EFT dimension-8 operators without and with applying an energy cut-off scale to the invariant mass $m_{Z\gamma}$

	WWWW	WWZZ	ZZZZ	WWAZ	WWAA	ZZZA	ZZAA	ZAAA	AAAA
$\mathcal{O}_{S,0}$, $\mathcal{O}_{S,1}$	X	X	X						
$\mathcal{O}_{M,0}$, $\mathcal{O}_{M,1}$,$\mathcal{O}_{M,6}$,$\mathcal{O}_{M,7}$	X	X	X	X	X	X	X		
$\mathcal{O}_{M,2}$,$\mathcal{O}_{M,3}$, $\mathcal{O}_{M,4}$,$\mathcal{O}_{M,5}$		X	X	X	X	X	X		
$\mathcal{O}_{T,0}$,$\mathcal{O}_{T,1}$,$\mathcal{O}_{T,2}$	X	X	X	X	X	X	X	X	X
$\mathcal{O}_{T,5}$,$\mathcal{O}_{T,6}$,$\mathcal{O}_{T,7}$		X	X	X	X	X	X	X	X
$\mathcal{O}_{T,8}$,$\mathcal{O}_{T,9}$			X			X	X	X	X

TABLE II: Quartic vertices modified by each dimension-8 operator are marked with X.

Coefficient	Observed limit [TeV^{-4}]	Expected limit [TeV^{-4}]
f_{T0}/Λ^4	$[-9.4, 8.4] \times 10^{-2}$	$[-1.3, 1.2] \times 10^{-1}$
f_{T5}/Λ^4	$[-8.8, 9.9] \times 10^{-2}$	$[-1.2, 1.3] \times 10^{-1}$
f_{T8}/Λ^4	$[-5.9, 5.9] \times 10^{-2}$	$[-8.1, 8.0] \times 10^{-2}$
f_{T9}/Λ^4	$[-1.3, 1.3] \times 10^{-1}$	$[-1.7, 1.7] \times 10^{-1}$
f_{M0}/Λ^4	$[-4.6, 4.6]$	$[-6.2, 6.2]$
f_{M1}/Λ^4	$[-7.7, 7.7]$	$[-1.0, 1.0] \times 10^{1}$
f_{M2}/Λ^4	$[-1.9, 1.9]$	$[-2.6, 2.6]$

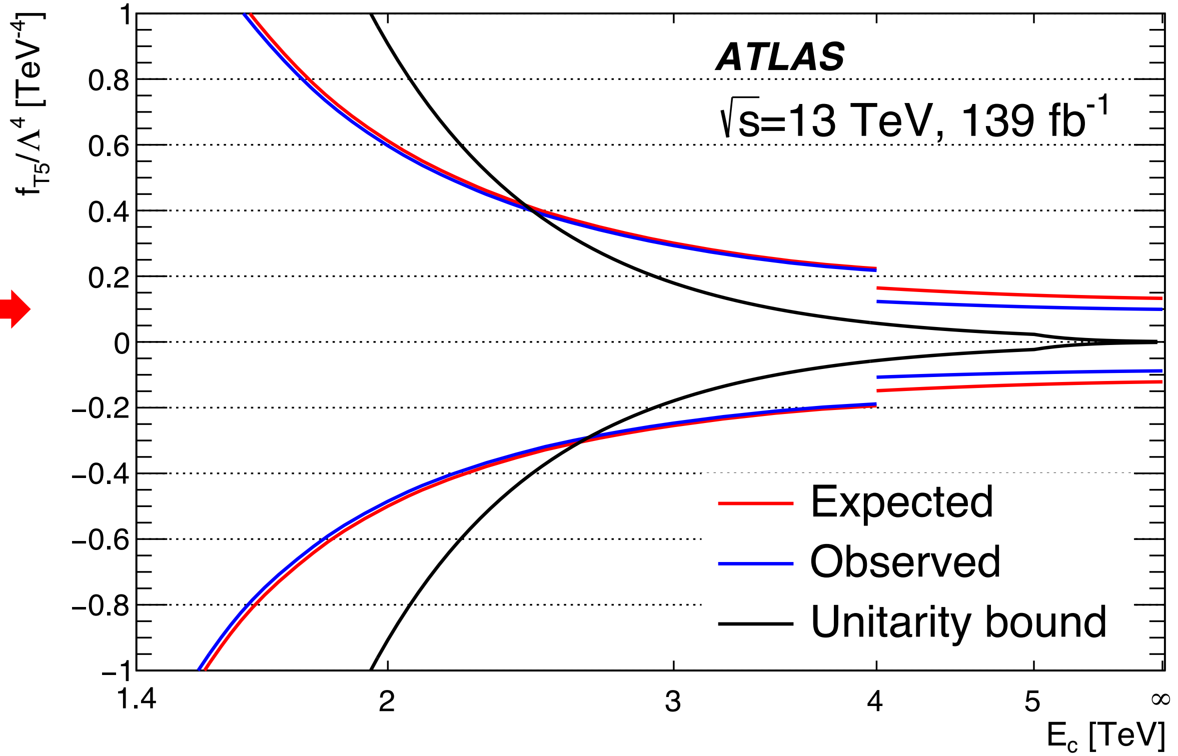

Summary

- Measurements of electroweak processes sensitive to vector boson scattering allow to test the gauge interactions of the SM electroweak theory and its symmetry breaking mechanism

- ATLAS public results of the electroweak VBS measurements using the full Run-2 dataset of proton-proton collisions collected at $\sqrt{s} = 13$ TeV were reviewed

- All presented results are consistent with the Standard Model predictions within the measurement uncertainties

- More VBS measurements using the full Run-2 dataset should be available for public this year

Tuesday 05.03., T.38: Standard model 1 (electroweak/bosons)

Thank you!

Content

- Electroweak vector boson self-interactions in the Standard Model
  - Vector boson scattering (VBS)

- VBS as a probe of the SM electroweak symmetry breaking mechanism

- Searches for anomalous quartic gauge couplings in VBS processes
  - Effective field theory (EFT) framework

- EWK VBS-sensitive measurements in the ATLAS detector using the full Run-2 dataset
  - Highlights of the measurement methods and results
    - Same sign $WWjj$, fully leptonic
    - ~~Opposite sign $WWjj$, fully leptonic~~
    - $ZZ(\rightarrow 4l)jj$
    - $Z(\rightarrow \nu\nu)\gamma jj$
    - ~~$Z(\rightarrow ll)\gamma jj$~~

140 fb^{-1} roton-proton collision data collected at $\sqrt{s} = 13$ TeV

- Summary

New Physics Searches – Anomalous Gauge Couplings

❑ Dimension-8 operators

$$\mathcal{O}_{S,0} = [(D_\mu\Phi)^\dagger D_\nu\Phi] \times [(D^\mu\Phi)^\dagger D^\nu\Phi]$$
$$\mathcal{O}_{S,1} = [(D_\mu\Phi)^\dagger D^\mu\Phi] \times [(D_\nu\Phi)^\dagger D^\nu\Phi]$$
$$\mathcal{O}_{S,2} = [(D_\mu\Phi)^\dagger D_\nu\Phi] \times [(D^\nu\Phi)^\dagger D^\mu\Phi]$$

$$D_\mu\Phi = (\partial_\mu + igW^j_\mu \tfrac{\sigma^j}{2} + ig' B_\mu \tfrac{1}{2})\Phi$$

$$\mathcal{O}_{M,0} = \mathrm{Tr}[\hat{W}_{\mu\nu}\hat{W}^{\mu\nu}] \times [(D_\beta\Phi)^\dagger D^\beta\Phi],$$
$$\mathcal{O}_{M,1} = \mathrm{Tr}[\hat{W}_{\mu\nu}\hat{W}^{\nu\beta}] \times [(D_\beta\Phi)^\dagger D^\mu\Phi],$$
$$\mathcal{O}_{M,2} = [B_{\mu\nu}B^{\mu\nu}] \times [(D_\beta\Phi)^\dagger D^\beta\Phi],$$
$$\mathcal{O}_{M,3} = [B_{\mu\nu}B^{\nu\beta}] \times [(D_\beta\Phi)^\dagger D^\mu\Phi],$$
$$\mathcal{O}_{M,4} = [(D_\mu\Phi)^\dagger \hat{W}_{\beta\nu} D^\mu\Phi] \times B^{\beta\nu},$$
$$\mathcal{O}_{M,5} = [(D_\mu\Phi)^\dagger \hat{W}_{\beta\nu} D^\nu\Phi] \times B^{\beta\mu} + \mathrm{H.c.},$$
$$\mathcal{O}_{M,7} = [(D_\mu\Phi)^\dagger \hat{W}_{\beta\nu}\hat{W}^{\beta\mu} D^\nu\Phi].$$

$$\hat{W}_{\mu\nu} \equiv W^j_{\mu\nu}\tfrac{\sigma^j}{2} \qquad \sigma^j\ (j = 1,\ 2,\ 3)$$

$$\mathcal{O}_{T,0} = \mathrm{Tr}[\hat{W}_{\mu\nu}\hat{W}^{\mu\nu}] \times \mathrm{Tr}[\hat{W}_{\alpha\beta}\hat{W}^{\alpha\beta}],$$
$$\mathcal{O}_{T,1} = \mathrm{Tr}[\hat{W}_{\alpha\nu}\hat{W}^{\mu\beta}] \times \mathrm{Tr}[\hat{W}_{\mu\beta}\hat{W}^{\alpha\nu}]$$
$$\mathcal{O}_{T,2} = \mathrm{Tr}[\hat{W}_{\alpha\mu}\hat{W}^{\mu\beta}] \times \mathrm{Tr}[\hat{W}_{\beta\nu}\hat{W}^{\nu\alpha}],$$
$$\mathcal{O}_{T,5} = \mathrm{Tr}[\hat{W}_{\mu\nu}\hat{W}^{\mu\nu}] \times B_{\alpha\beta}B^{\alpha\beta}$$
$$\mathcal{O}_{T,6} = \mathrm{Tr}[\hat{W}_{\alpha\nu}\hat{W}^{\mu\beta}] \times B_{\mu\beta}B^{\alpha\nu},$$
$$\mathcal{O}_{T,7} = \mathrm{Tr}[\hat{W}_{\alpha\mu}\hat{W}^{\mu\beta}] \times B_{\beta\nu}B^{\nu\alpha}$$
$$\mathcal{O}_{T,8} = B_{\mu\nu}B^{\mu\nu}B_{\alpha\beta}B^{\alpha\beta}, \qquad \mathcal{O}_{T,9} = B_{\alpha\mu}B^{\mu\beta}B_{\beta\nu}B^{\nu\alpha}.$$

	WWWW	WWZZ	ZZZZ	WWAZ	WWAA	ZZZA	ZZAA	ZAAA	AAAA
$\mathcal{O}_{S,0}$, $\mathcal{O}_{S,1}$	X	X	X						
$\mathcal{O}_{M,0}$, $\mathcal{O}_{M,1}$, $\mathcal{O}_{M,6}$, $\mathcal{O}_{M,7}$	X	X	X	X	X	X	X		
$\mathcal{O}_{M,2}$, $\mathcal{O}_{M,3}$, $\mathcal{O}_{M,4}$, $\mathcal{O}_{M,5}$		X	X	X	X	X	X		
$\mathcal{O}_{T,0}$, $\mathcal{O}_{T,1}$, $\mathcal{O}_{T,2}$	X	X	X	X	X	X	X	X	X
$\mathcal{O}_{T,5}$, $\mathcal{O}_{T,6}$, $\mathcal{O}_{T,7}$		X	X	X	X	X	X	X	X
$\mathcal{O}_{T,8}$, $\mathcal{O}_{T,9}$			X			X	X	X	X

TABLE II: Quartic vertices modified by each dimension-8 operator are marked with X.

Same Sign $W^{\pm}W^{\pm}jj$ Measurement

- Monte-Carlo signal and background samples

Process, short description	ME Generator + parton shower	Order	Tune	PDF set in ME
EW, Int, QCD $W^{\pm}W^{\pm}jj$, nominal signal	MadGraph5_aMC@NLO2.6.7 + Herwig7.2	LO	Herwig	NNPDF3.0nlo
EW, Int, QCD $W^{\pm}W^{\pm}jj$, alternative shower	MadGraph5_aMC@NLO2.6.7 + Pythia8.244	LO	A14	NNPDF3.0nlo
EW $W^{\pm}W^{\pm}jj$, NLO pQCD approx.	Sherpa2.2.11 & Sherpa2.2.2(WWW) & Powheg Box2+Pythia8.235 (WH)	+0,1j@LO NLO	Sherpa A14	NNPDF3.0nnlo
EW $W^{\pm}W^{\pm}jj$, NLO pQCD approx.	Powheg Boxv2 + Pythia8.230	NLO (VBS approx.)	AZNLO	NNPDF3.0nlo
QCD $W^{\pm}W^{\pm}jj$, NLO pQCD approx.	Sherpa2.2.2	+0,1j@LO	Sherpa	NNPDF3.0nnlo
QCD $VVjj$	Sherpa2.2.2	+0,1j@NLO; +2,3j@LO	Sherpa	NNPDF3.0nnlo
EW $W^{\pm}Z/\gamma^{*}jj$	MadGraph5_aMC@NLO2.6.2+Pythia8.235	LO	A14	NNPDF3.0nlo
EW $Z/\gamma^{*}Z/\gamma^{*}jj$	Sherpa2.2.2	LO	Sherpa	NNPDF3.0nnlo
QCD $V\gamma jj$	Sherpa2.2.11	+0,1j@NLO; +2,3j@LO	A14	NNPDF3.0nnlo
EW $V\gamma jj$	MadGraph5_aMC@NLO2.6.5+Pythia8.240	LO	A14	NNPDF3.0nlo
VVV	Sherpa2.2.1 (leptonic) & Sherpa2.2.2 (one $V \rightarrow jj$)	+0,1j@LO	Sherpa	NNPDF3.0nnlo
$t\bar{t}V$	MadGraph5_aMC@NLO2.3.3.p0 + Pythia8.210	NLO	A14	NNPDF3.0nlo
tZq	MadGraph5_aMC@NLO2.3.3.p1 + Pythia8.212	LO	A14	NNPDF2.3lo
$W^{\pm}W^{\pm}jj$ EFT	MadGraph5_aMC@NLO 2.6.5 + Pythia8.235	LO	A14	NNPDF3.0nlo
$\mathrm{H}_5^{\pm\pm}$	MadGraph5_aMC@NLO 2.9.5 + Pythia8.245	LO	A14	NNPDF3.0nlo

Same Sign $W^{\pm}W^{\pm}jj$ Measurement

- ❑ Event selection signal and control regions

Requirement	SR	Low-m_{jj} CR	WZ CR
Leading and subleading lepton p_{T}	> 27 GeV		
Electron $\|\eta\|$	< 2.47 (1.37 in ee), excluding $1.37 \leq \|\eta\| \leq 1.52$		
Muon $\|\eta\|$	< 2.5		
Leading (subleading) jet p_{T}	$> 65\,(35)$ GeV		
Additional jet p_{T}	> 25 GeV		
Jet $\|\eta\|$	< 4.5		
$m_{\ell\ell}$	> 20 GeV		
$E_{\mathrm{T}}^{\mathrm{miss}}$	> 30 GeV		
Charge misid. $Z \to ee$ veto	$\|m_{ee} - m_Z\| > 15$ GeV		–
b-jet veto	$N_{b\text{-jet}} = 0$, $p_{\mathrm{T}}^{b\text{-jet}} > 20$ GeV, $\|\eta^{b\text{-jet}}\| < 2.5$		
$N_{\mathrm{veto\ leptons}}$	$= 0$	$= 0$	$= 1\,, p_{\mathrm{T}} > 15$ GeV
$m_{\ell\ell\ell}$	–	–	> 106 GeV
m_{jj}	> 500 GeV	$200 < m_{\mathrm{jj}} < 500$ GeV	> 200 GeV
$\|\Delta y_{\mathrm{jj}}\|$	> 2		

Same Sign $W^{\pm}W^{\pm}jj$ Measurement

- Differential cross section messurement with profile-likelihood unfolding
  - Post-fit distributions obtained in the fit of differential cross section as a function of m_{ll}
    - Signal from different particle-level m_{ll} slices (numbered in brackets) is shown in different shades of blue

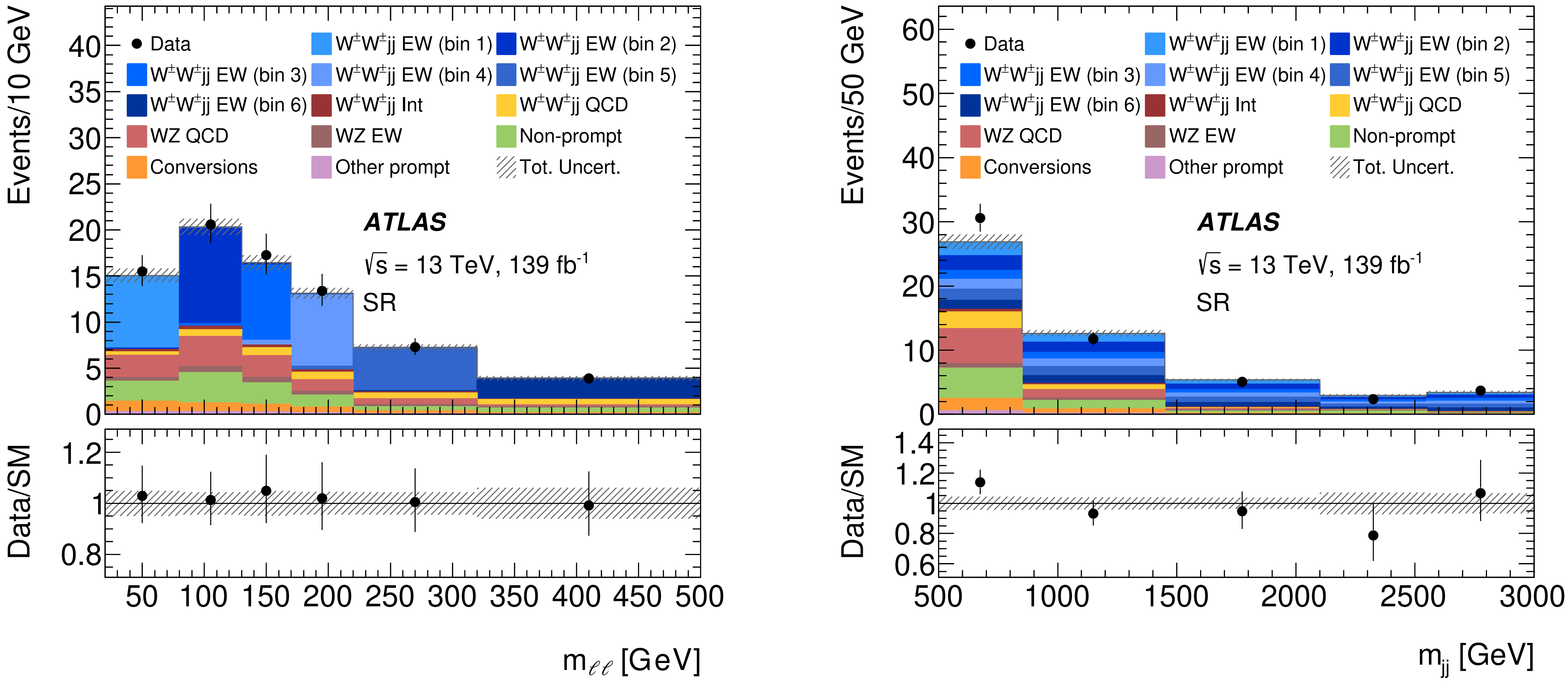

Same Sign $W^{\pm}W^{\pm}jj$ Measurement

- ❑ Differential cross sections obtained using the profile-likelihood unfolding method

$$m_{\mathrm{T}} = \sqrt{\left(E_{\mathrm{T}}^{\ell\ell} + E_{\mathrm{T}}^{\mathrm{miss}}\right)^2 - \left|\vec{p}_{\mathrm{T}}^{\,\ell\ell} + \vec{E}_{\mathrm{T}}^{\mathrm{miss}}\right|^2}$$

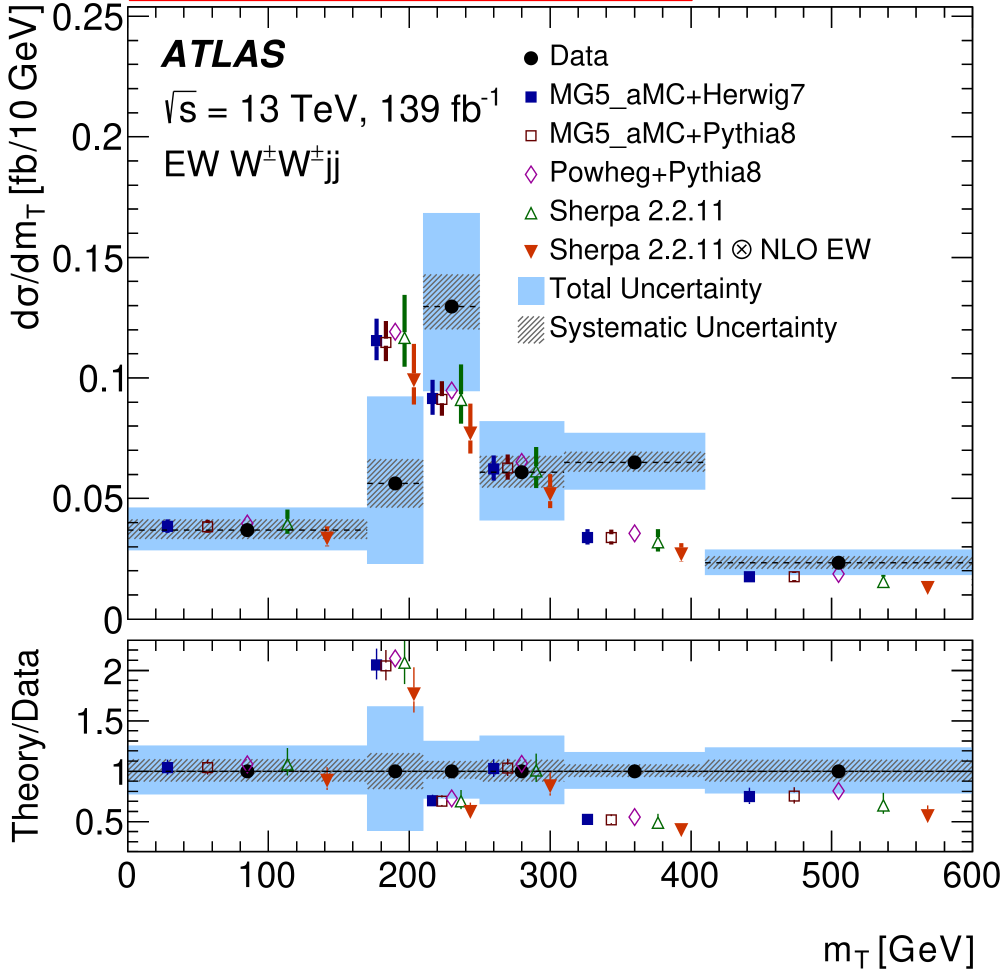

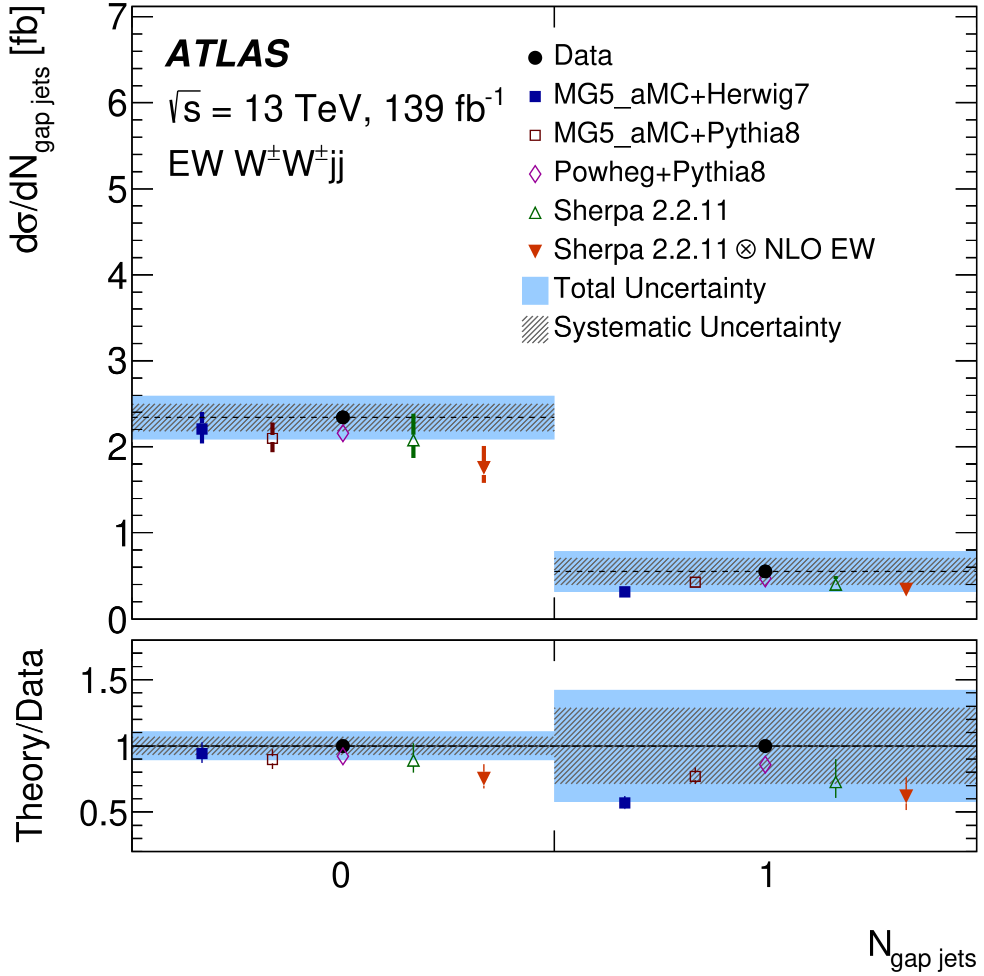

Same Sign $W^{\pm}W^{\pm}jj$ Measurement

- Differential cross sections obtained using the profile-likelihood unfolding method

$$\xi_{j3} = \left| \frac{\eta_{j3} - \frac{1}{2}(\eta_{j1} + \eta_{j2})}{\eta_{j2} - \eta_{j1}} \right|$$

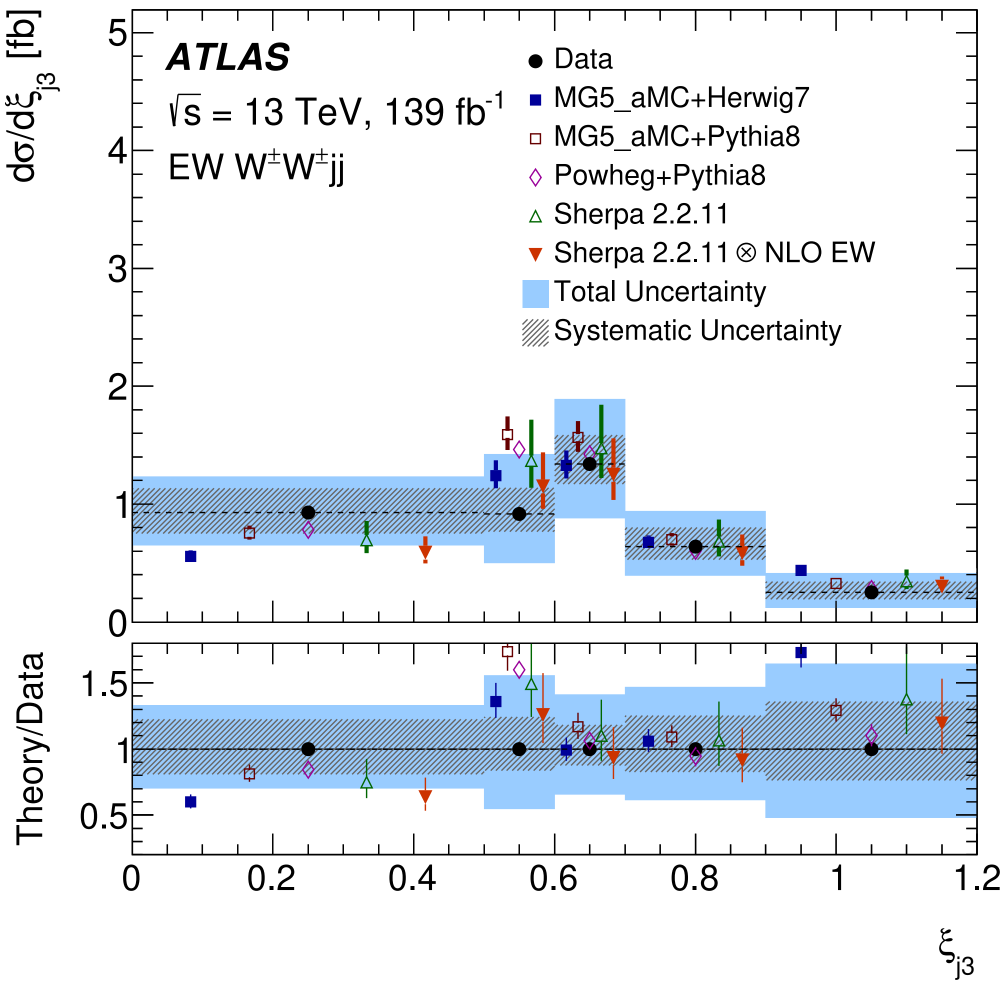

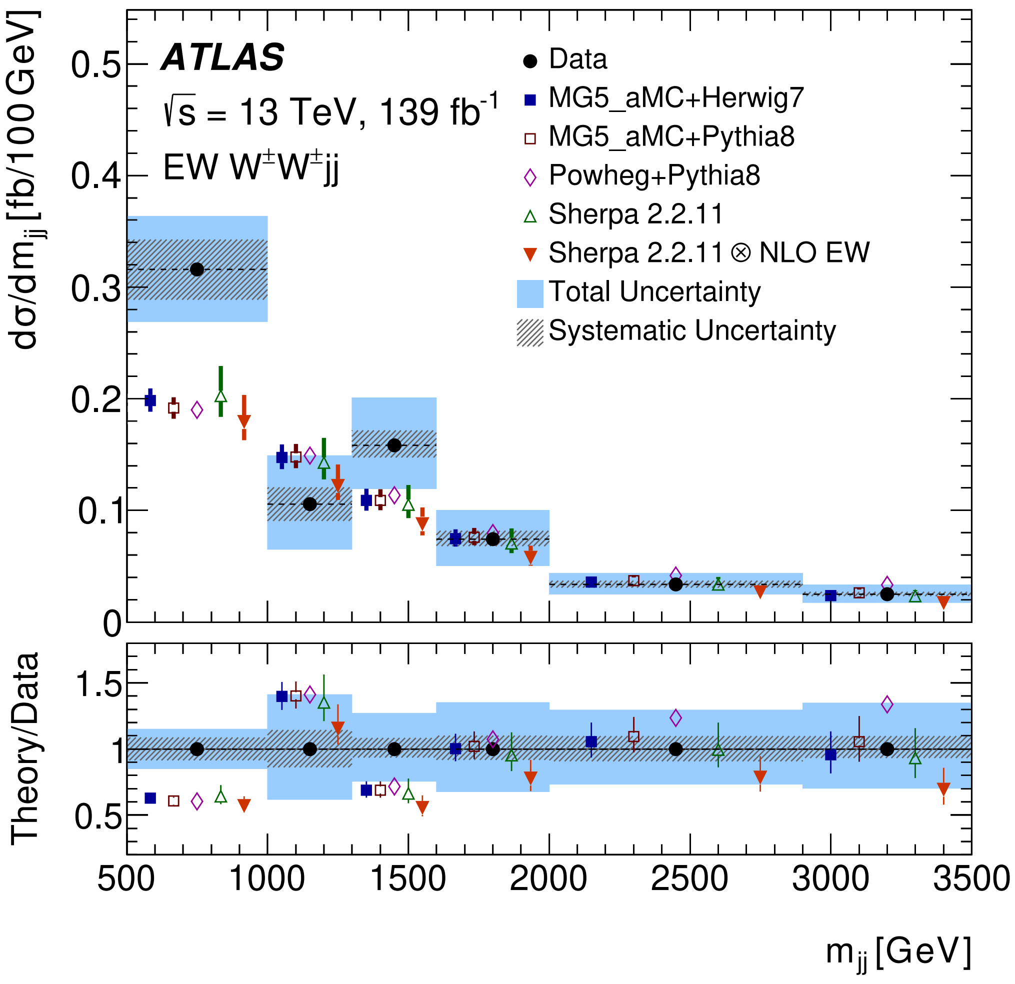

Same Sign $W^{\pm}W^{\pm}jj$ Measurement

- ❑ Search for the doubly charged Higgs boson of the GM (Georgi and Machacek) model
- ❑ Excess observed at $m_T = 450$ GeV with the local (global) significance of 3.3σ (2.5σ)

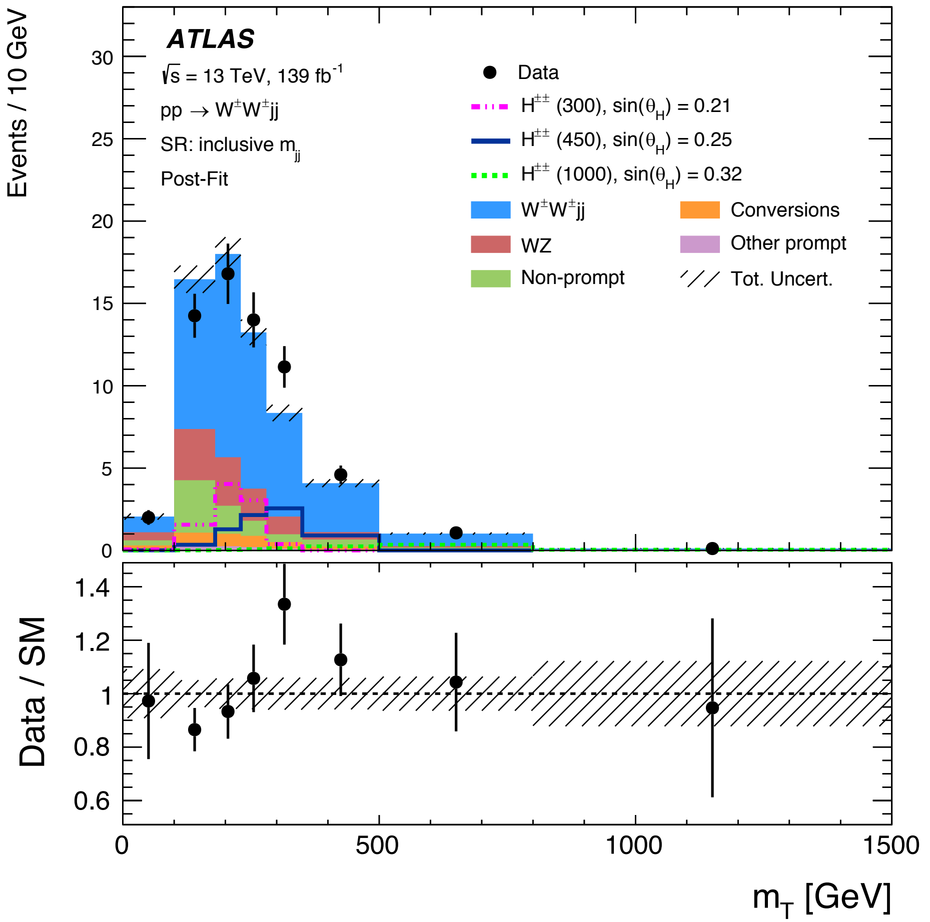

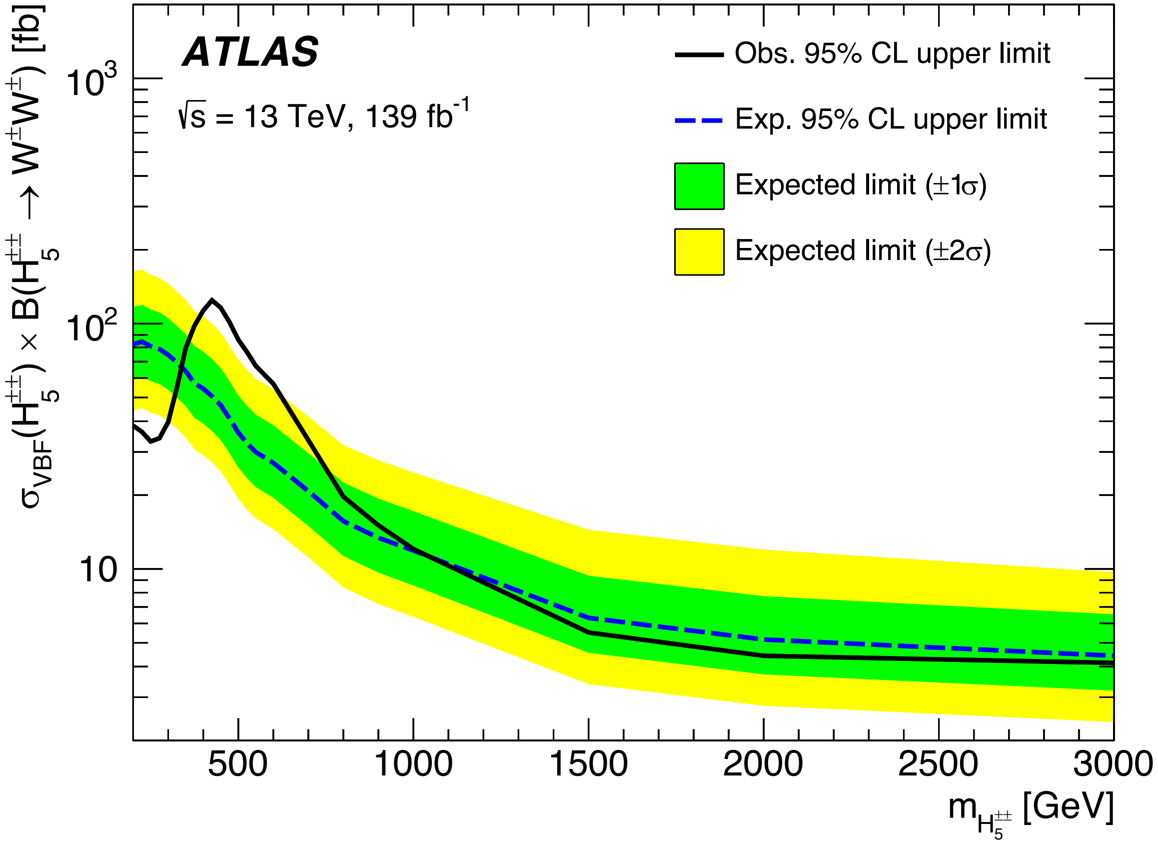

Same Sign $W^{\pm}W^{\pm}jj$ Measurement

- To dimensional scan for limits in the fit with contributions of two different EFT operators to the SM signal

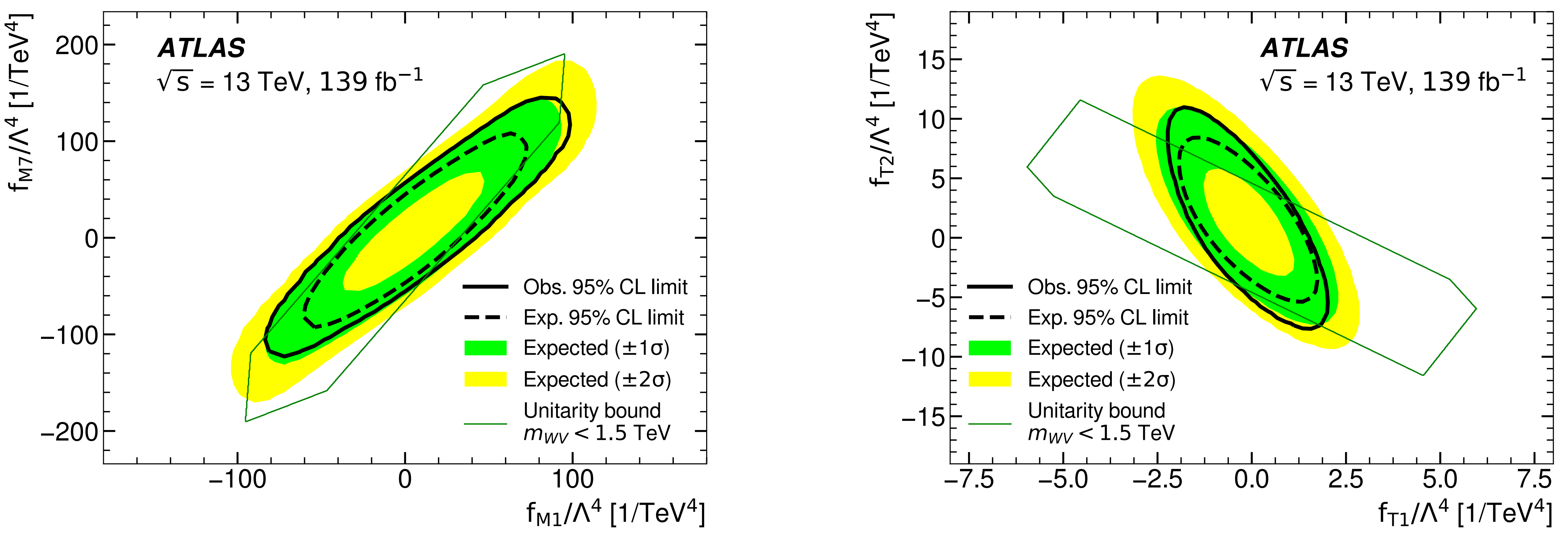

Prospects of $W^{\pm}W^{\pm}jj$ Measurement at HL-LHC

- 6-7% total uncertainty in the cross-section measurement at 3000 fb^{-1}
- Expected significance of the $W_L^{\pm}W_L^{\pm}$ VBS production at 3000 fb^{-1} : 1.8σ
  - ✦ CMS expects 2.7σ at the same integrated luminosity

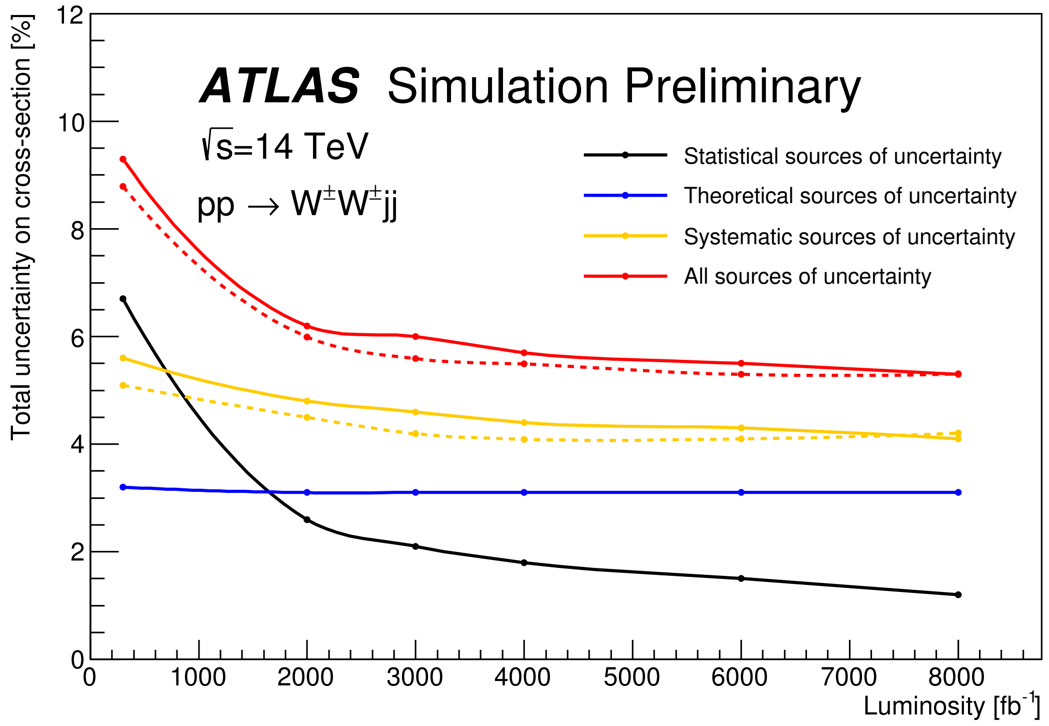

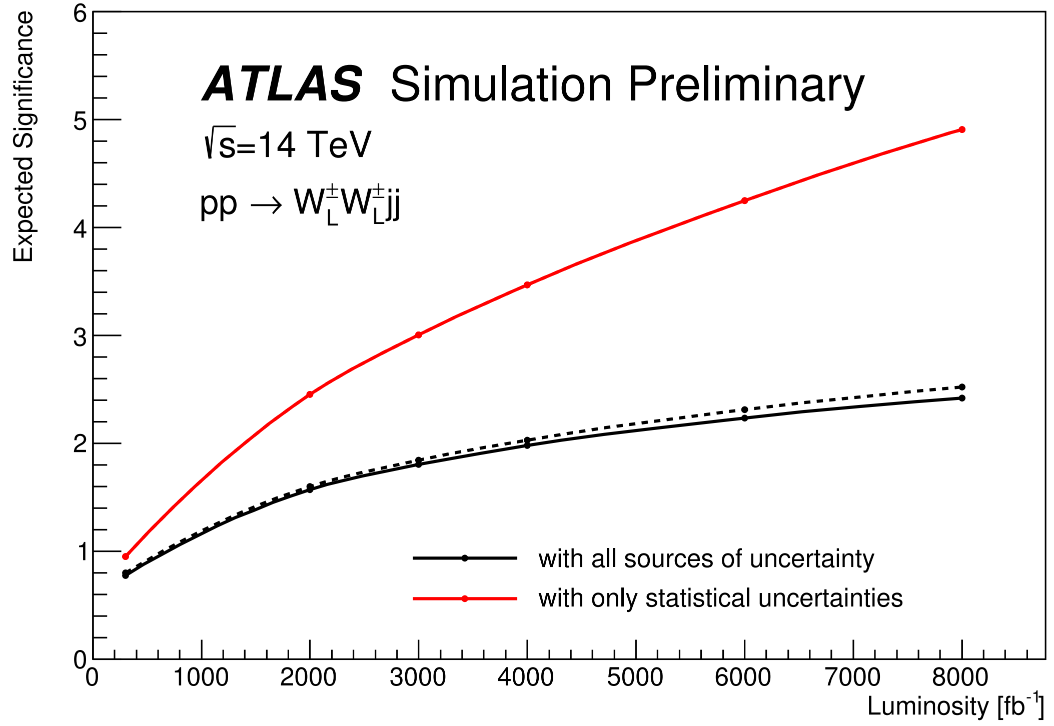

Observation of Opposite Sign W^+W^-jj

ATLAS-CONF-2023-039

$\sqrt{s} = 13\,TeV,\ 140\,fb^{-1}$

- ATLAS observed the electroweak VBS W^+W^-jj production in fully leptonic final states
  - Leptons are required to have different flavours

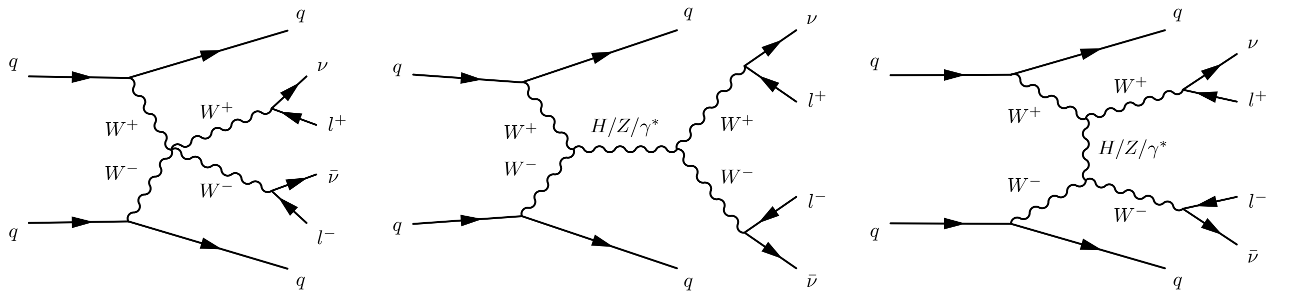

- Top quark (mainly the $t\bar{t}$) along with QCD W^+W^-jj production make huge background to the signal
  - 66% and 24% contributions to the total (post-fit) event prediction in the inclusive signal region, respectively, in contrast with **3% signal contribution**

Process	Event yields $n_{\text{jets}} = 2$	Event yields $n_{\text{jets}} = 3$
EWK $\mathrm{W^+W^-}jj$	158 ± 27	54 ± 13
Top quark	2885 ± 214	1851 ± 131
Strong $\mathrm{W^+W^-}jj$	1214 ± 256	514 ± 121
W+jets	37 ± 97	19 ± 48
Z+jets	216 ± 62	65 ± 25
Multiboson	101 ± 5	42 ± 3
SM prediction	4610 ± 77	2546 ± 48
Data	4610	2533

- Signal region is split into the exclusive 2- and 3-jet event categories to enhance the sensitivity

- Control region for the top quark background combines 2- and 3-jet events and is defined by requiring one of the two leading jets to be b-tagged

Observation of Opposite Sign W^+W^-jj

- Neural Network (TMVA) is trained separately in the 2- and 3-jet signal regions
  - Signal, top quark and QCD background events are used in the NN training
- Profile-likelihood fit method is used to fit simultaneously the signal, top and QCD background normalisations in the NN output in 1 control and 2 signal regions
- Observed (expected) signal significance is **7.1σ (6.2σ)**
  - Statistical uncertainty of the measured signal normalisation is **12.3%** with **18.5%** total uncertainty

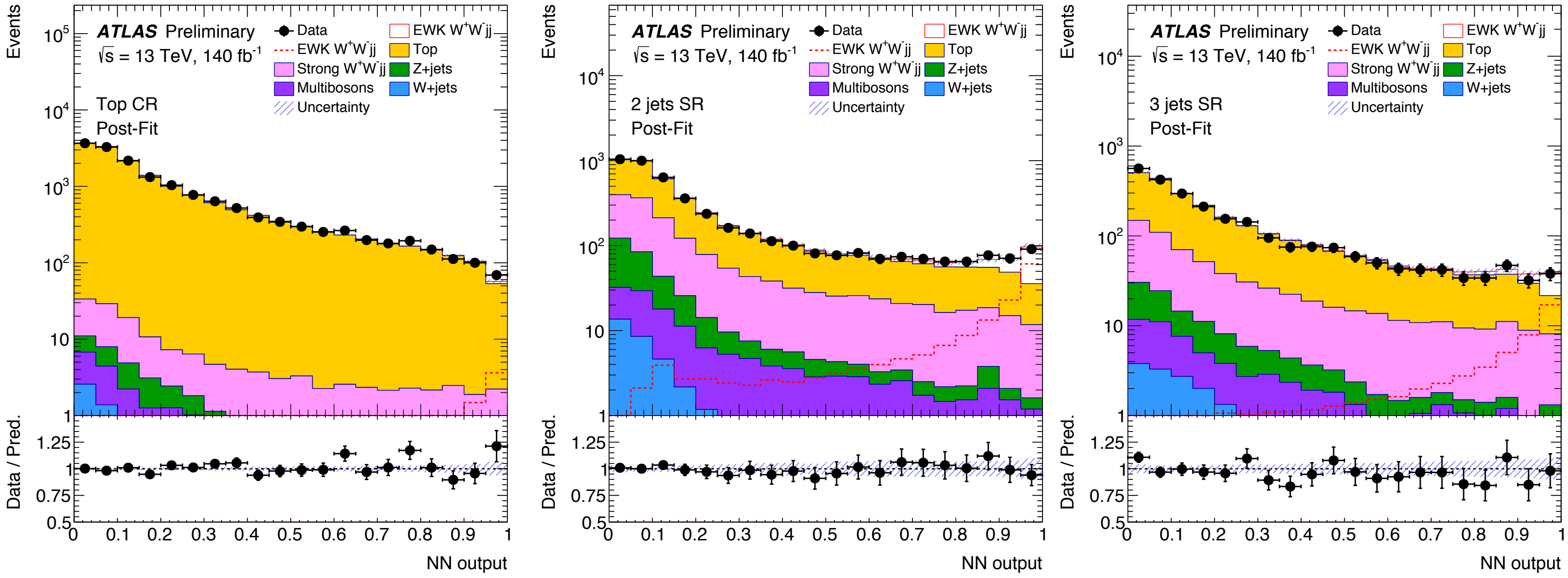

- Signal fiducial cross section is measured to $\mathbf{2.65^{+0.52}_{-0.48}}\ \boldsymbol{fb}$ vs. predicted $\mathbf{2.20^{+0.14}_{-0.13}}\ \boldsymbol{fb}$
  - Fiducial volume defined closely to detector level selection but requiring $m_{jj} > 500\ GeV$

Observation of Opposite Sign W^+W^-jj

- Object and event selection for the signal region at the detector level (left) and the definition of the measurement fiducial region at the particle level (right)

Category	Requirements
Leptons	$p_T > 27\,GeV$ $\lvert\eta\rvert < 2.47$ excluding $1.37 < \lvert\eta\rvert < 1.52$ (electrons) $\lvert\eta\rvert < 2.5$ (muons) Identification: `TightLH` (electrons), `Tight` (muons) Isolation: `Gradient` (electrons), `Tight_FixedRad` (muons) $\lvert d_0/\sigma_{d_0}\rvert < 5$ (electrons), $\lvert d_0/\sigma_{d_0}\rvert < 3$ (muons) $\lvert z_0 \sin\theta\rvert < 0.5\,\mathrm{mm}$
b-jets	$p_T > 20\,GeV$ and $\lvert\eta\rvert < 2.5$ (`DL1r` b-tagging with 85% efficiency)
Jets	$p_T > 25\,GeV$ and $\lvert\eta\rvert < 4.5$
Events	One electron and one muon with opposite electric charges No additional lepton with $p_T > 10\,GeV$, `Loose` isolation, `TightLH`/`MediumLH` (electrons) and `Loose` (muons) identification $\zeta > 0.5$ $m_{e\mu} > 80\,GeV$ $E_T^{miss} > 15\,GeV$ Two or three jets No b-jet

Category	Requirements
Leptons	$p_T > 27\,GeV$ and $\lvert\eta\rvert < 2.5$
b-jets	$p_T > 20\,GeV$ and $\lvert\eta\rvert < 2.5$
Jets	$p_T > 25\,GeV$ and $\lvert\eta\rvert < 4.5$
Events	One electron and one muon with opposite electric charges No additional lepton $\zeta > 0.5$ $m_{e\mu} > 80\,GeV$ $E_T^{miss} > 15\,GeV$ Two or three jets no b-jet $m_{jj} > 500\,GeV$

EFT Limits on Coefficients of Dimension-8 Operators

- ss $WWjj$ (left) and $ZZjj$ in 4 leptons final state (right)

Coefficient	Type	No unitarisation cut-off [TeV^{-4}]	Lower, upper limit at the respective unitarity bound [TeV^{-4}]
f_{M0}/Λ^4	Exp.	[-3.9, 3.8]	-64 at 0.9 TeV, 40 at 1.0 TeV
	Obs.	[-4.1, 4.1]	-140 at 0.7 TeV, 117 at 0.8 TeV
f_{M1}/Λ^4	Exp.	[-6.3, 6.6]	-25.5 at 1.6 TeV, 31 at 1.5 TeV
	Obs.	[-6.8, 7.0]	-45 at 1.4 TeV, 54 at 1.3 TeV
f_{M7}/Λ^4	Exp.	[-9.3, 8.8]	-33 at 1.8 TeV, 29.1 at 1.8 TeV
	Obs.	[-9.8, 9.5]	-39 at 1.7 TeV, 42 at 1.7 TeV
f_{S02}/Λ^4	Exp.	[-5.5, 5.7]	-94 at 0.8 TeV, 122 at 0.7 TeV
	Obs.	[-5.9, 5.9]	–
f_{S1}/Λ^4	Exp.	[-22.0, 22.5]	–
	Obs.	[-23.5, 23.6]	–
f_{T0}/Λ^4	Exp.	[-0.34, 0.34]	-3.2 at 1.2 TeV, 4.9 at 1.1 TeV
	Obs.	[-0.36, 0.36]	-7.4 at 1.0 TeV, 12.4 at 0.9 TeV
f_{T1}/Λ^4	Exp.	[-0.158, 0.174]	-0.32 at 2.6 TeV, 0.44 at 2.4 TeV
	Obs.	[-0.174, 0.186]	-0.38 at 2.5 TeV, 0.49 at 2.4 TeV
f_{T2}/Λ^4	Exp.	[-0.56, 0.70]	-2.60 at 1.7 TeV, 10.3 at 1.2 TeV
	Obs.	[-0.63, 0.74]	–

Wilson coefficient	$\lvert\mathcal{M}_{d8}\rvert^2$ Included	95% confidence interval [TeV^{-4}] Expected	Observed
$f_{T,0}/\Lambda^4$	yes	[-0.98, 0.93]	[-1.00, 0.97]
	no	[-23, 17]	[-19, 19]
$f_{T,1}/\Lambda^4$	yes	[-1.2, 1.2]	[-1.3, 1.3]
	no	[-160, 120]	[-140, 140]
$f_{T,2}/\Lambda^4$	yes	[-2.5, 2.4]	[-2.6, 2.5]
	no	[-74, 56]	[-63, 62]
$f_{T,5}/\Lambda^4$	yes	[-2.5, 2.4]	[-2.6, 2.5]
	no	[-79, 60]	[-68, 67]
$f_{T,6}/\Lambda^4$	yes	[-3.9, 3.9]	[-4.1, 4.1]
	no	[-64, 48]	[-55, 54]
$f_{T,7}/\Lambda^4$	yes	[-8.5, 8.1]	[-8.8, 8.4]
	no	[-260, 200]	[-220, 220]
$f_{T,8}/\Lambda^4$	yes	[-2.1, 2.1]	[-2.2, 2.2]
	no	[-4.6, 3.1]$\times 10^4$	[-3.9, 3.8]$\times 10^4$
$f_{T,9}/\Lambda^4$	yes	[-4.5, 4.5]	[-4.7, 4.7]
	no	[-7.5, 5.5]$\times 10^4$	[-6.4, 6.3]$\times 10^4$

EFT Limits on Coefficients of Dimension-8 Operators

- ss $WWjj$ (top) and $Z(\nu\nu)\gamma$jj (bottom)

Coefficient	Type	No unitarisation cut-off [TeV^{-4}]	Lower, upper limit at the respective unitarity bound [TeV^{-4}]
f_{M0}/Λ^4	Exp.	[-3.9, 3.8]	-64 at 0.9 TeV, 40 at 1.0 TeV
	Obs.	[-4.1, 4.1]	-140 at 0.7 TeV, 117 at 0.8 TeV
f_{M1}/Λ^4	Exp.	[-6.3, 6.6]	-25.5 at 1.6 TeV, 31 at 1.5 TeV
	Obs.	[-6.8, 7.0]	-45 at 1.4 TeV, 54 at 1.3 TeV
f_{M7}/Λ^4	Exp.	[-9.3, 8.8]	-33 at 1.8 TeV, 29.1 at 1.8 TeV
	Obs.	[-9.8, 9.5]	-39 at 1.7 TeV, 42 at 1.7 TeV
f_{S02}/Λ^4	Exp.	[-5.5, 5.7]	-94 at 0.8 TeV, 122 at 0.7 TeV
	Obs.	[-5.9, 5.9]	–
f_{S1}/Λ^4	Exp.	[-22.0, 22.5]	–
	Obs.	[-23.5, 23.6]	–
f_{T0}/Λ^4	Exp.	[-0.34, 0.34]	-3.2 at 1.2 TeV, 4.9 at 1.1 TeV
	Obs.	[-0.36, 0.36]	-7.4 at 1.0 TeV, 12.4 at 0.9 TeV
f_{T1}/Λ^4	Exp.	[-0.158, 0.174]	-0.32 at 2.6 TeV, 0.44 at 2.4 TeV
	Obs.	[-0.174, 0.186]	-0.38 at 2.5 TeV, 0.49 at 2.4 TeV
f_{T2}/Λ^4	Exp.	[-0.56, 0.70]	-2.60 at 1.7 TeV, 10.3 at 1.2 TeV
	Obs.	[-0.63, 0.74]	–

Coefficient	Observed limit [TeV^{-4}]	Expected limit [TeV^{-4}]
f_{T0}/Λ^4	$[-9.4, 8.4]\times10^{-2}$	$[-1.3, 1.2]\times10^{-1}$
f_{T5}/Λ^4	$[-8.8, 9.9]\times10^{-2}$	$[-1.2, 1.3]\times10^{-1}$
f_{T8}/Λ^4	$[-5.9, 5.9]\times10^{-2}$	$[-8.1, 8.0]\times10^{-2}$
f_{T9}/Λ^4	$[-1.3, 1.3]\times10^{-1}$	$[-1.7, 1.7]\times10^{-1}$
f_{M0}/Λ^4	$[-4.6, 4.6]$	$[-6.2, 6.2]$
f_{M1}/Λ^4	$[-7.7, 7.7]$	$[-1.0, 1.0]\times10^{1}$
f_{M2}/Λ^4	$[-1.9, 1.9]$	$[-2.6, 2.6]$

Coefficient	E_c [TeV]	Observed limit [TeV^{-4}]	Expected limit [TeV^{-4}]
f_{T0}/Λ^4	1.7	$[-8.7, 7.1]\times10^{-1}$	$[-8.9, 7.3]\times10^{-1}$
f_{T5}/Λ^4	2.4	$[-3.4, 4.2]\times10^{-1}$	$[-3.5, 4.3]\times10^{-1}$
f_{T8}/Λ^4	1.7	$[-5.2, 5.2]\times10^{-1}$	$[-5.3, 5.3]\times10^{-1}$
f_{T9}/Λ^4	1.9	$[-7.9, 7.9]\times10^{-1}$	$[-8.1, 8.1]\times10^{-1}$
f_{M0}/Λ^4	0.7	$[-1.6, 1.6]\times10^{2}$	$[-1.5, 1.5]\times10^{2}$
f_{M1}/Λ^4	1.0	$[-1.6, 1.5]\times10^{2}$	$[-1.4, 1.4]\times10^{2}$
f_{M2}/Λ^4	1.0	$[-3.3, 3.2]\times10^{1}$	$[-3.0, 3.0]\times10^{1}$

$Z(\rightarrow ll)\gamma jj$ Measurement

[Phys. Lett. B 846 (2023) 138222]

$\sqrt{s} = 13\,TeV,\ 140\,fb^{-1}$

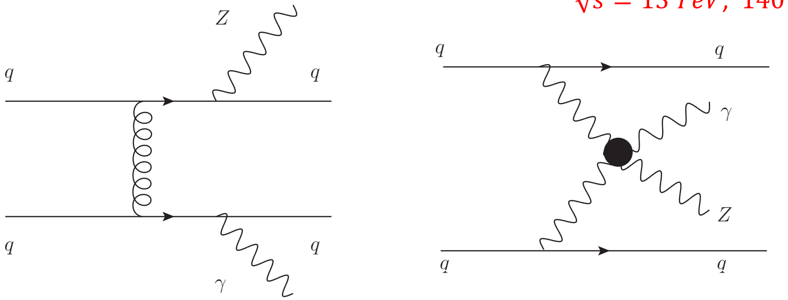

- EW (sensitive to VBS) and extended EW (EW+QCD) production fiducial and differential cross sections are measured in leptonic final states, ee and $\mu\mu$
  - The EW measurements employ a control region to constrain the QCD background
    - SR: $\boldsymbol{\zeta(Z\gamma) < 0.4}$, CR: $\boldsymbol{\zeta(Z\gamma) > 0.4}$

$$\zeta(Z\gamma) = \left|\frac{y_{Z\gamma} - (y_{j_1} + y_{j_2})/2}{y_{j_1} - y_{j_2}}\right|$$

- Profile-likelihood fit to m_{jj} distributions in the SR and CR (in case of the EW measurement) is used to extract signal normalisation → evaluate fiducial cross sections
  - Both EW and extended EW fiducial cross sections are in a good agreement with the SM predictions

EW ($m_{jj} > 500\ GeV$): $\sigma_{\text{EW}} = 3.6 \pm 0.5$ fb, $\sigma_{\text{EW}}^{pred} = 3.5 \pm 0.2$ fb

Extended EW ($m_{jj} > 150\ GeV$): $\sigma_{Z\gamma} = 16.8^{+2.0}_{-1.8}$ fb, $\sigma_{Z\gamma}^{pred} = 15.7^{+5.0}_{-2.6}$ fb

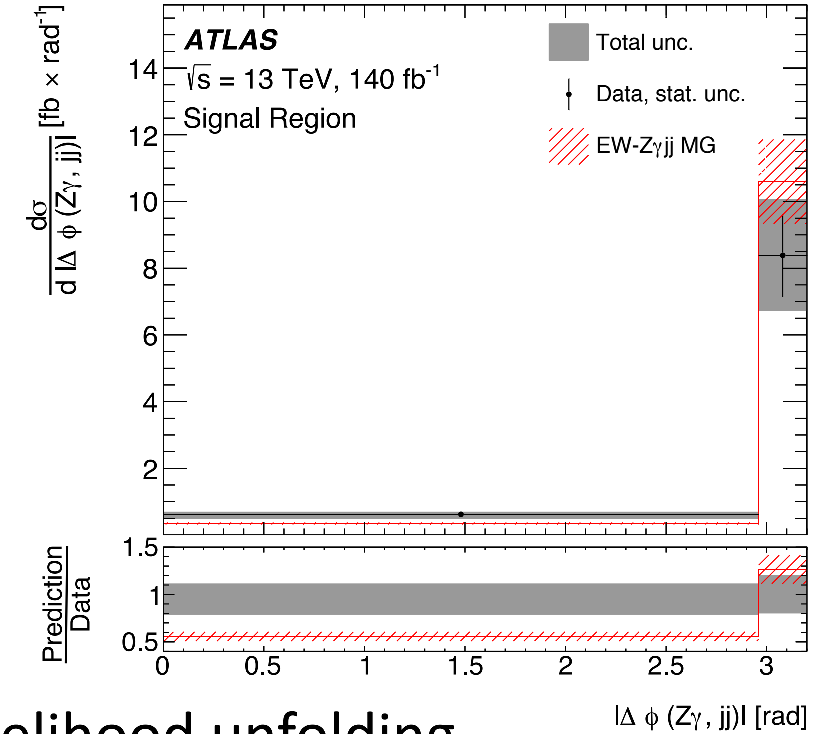

- Differential cross sections are measured using profile-likelihood unfolding
  - Unfolded observables are in a good agreement with SM distributions except of $|\Delta\boldsymbol{\phi}(\boldsymbol{Z\gamma}, \boldsymbol{jj})|$
    - About two standard deviation is observed in the lowest bin of the EW measurement